Klinikum rechts der Isar
der Technischen Universität München
Lehrstuhl für Klinische Chemie

The role of MALT1 in ITK-SYK mediated lymphomagenesis

Ines Vera Rechenberger

Vollständiger Abdruck der von der Fakultät für Medizin der Technischen Universität München zur Erlangung des akademischen Grades eines Doktors der Medizin genehmigten Dissertation.

Vorsitzender: Prof. Dr. Ernst J. Rummeny

Prüfer der Dissertation:

1. Prof. Dr. Jürgen Ruland
2. Prof. Dr. Angela Krackhardt

Die Dissertation wurde am 06.06.2017 bei der Technischen Universität München eingereicht und durch die Fakultät für Medizin am 28.03.2018 angenommen.

To

Katharina Sophia Maria Gensbaur

(1988 – 1993)

1 Table of Content

2 List of abbreviations

Instance	Expansion
%	per cent
>	more than
<	less than
°C	degree Celsius
7AAD	7-amino-actinomycin D
A	ampere/ deoxyadenylate
ABC	Activated B-cell
AF	alexa fluor
ALCL	anaplastic large cell lymphoma
AP-1	activator protein-1
APC	allophycocyanin
BCL	B-cell lymphoma
BCR	B-cell receptor
C	deoxycytidylate
CARD	caspase activation and recruitment domain
CARMA	CARD-containing MAGUK protein
CBM	CARMA1/BCL10/MALT1
CD	cluster of differentiation
CHOP	Cyclophosphamide, Hydroxydaunorubicin, Oncovin (Vincristine), Prednisone
CPD	Cell Proliferation Dye
Cre	causes recombination

DAG	diacylglycerol
DD	death domain
dest.	destillata
DN	double negative
DNA	deoxyribonucleic acid
dNTP	deoxyribonucleotide triphosphate
DP	double positive
EDTA	ethylenediaminetetraacetic acid
eGFP	enhanced green fluorescent protein
ESS	Easycoll Separating Solution
FACS	Fluorescence-activated cell sorting
FCS	Fetal Calf Serum
Fig	figure
FSC	forward scatter
fwd	forward
G	deoxyguanylate
g	gram
h	hour(s)
Ig	immunoglobulin
IKK	inhibitor of kappa B kinase
IL	interleukin
IP_3	inositol (1,4,5)-trisphosphate
IRES	internal ribosomal entry site
ITAMs	immunoreceptor tyrosine-based activation motives

ITK	interleukin-2- inducible T-cell kinase
IκB	inhibitor of kappa B
l	litre
LAT	linker of activated T-cells
LCK	lymphocyte-specific protein tyrosine kinase
LED	Light Emitting Diode
m	milli
M	Mol
MAGUK	membrane-associated guanylate kinases
MALT1	mucosa associated lymphatic tissue 1
MAPK	mitogen-activated protein kinases
MHC	Major Histocompatibility Complex
min.	minutes
mM	milliMolar
N	number/ nano
NEMO	NF-kappa-B essential modulator
NFAT	nuclear factor of activated T-cells
NF-κB	nuclear factor kappa-light-chain-enhancer of activated B-cells
NHL	Non-Hodgkin lymphoma
NK	Natural Killer
ns	not significant
PBS	Phosphate buffered saline
PCR	polymerase chain reaction
Pe	phycoerythrin

PH	pleckstrin homology
PI3K	phosphatidylinositol-4,5-bisphosphate 3-kinase
PIP_2	phosphatidylinositol-4,5-bisphosphate
PIP_3	phosphatidylinositol-3,4,5-trisphosphate
PKC	protein kinase C
PLC	phospholipase C
PTCL	Peripheral T-cell lymphoma
PTCL-NOS	Peripheral T-cell lymphoma-not otherwise specified
PVP	polyvinylpyrrolidone
RAS	rat sarcoma
RBC	Red Blood Cell
Rel	related proteins
rev	reverse
RNA	ribonucleic acid
rpm	rounds per minute
RT	room temperature
SH2	src-homology 2
SLP-76	SH2 domain containing leukocyte protein of 76kDa
SP	single positive
Src	sarcoma
SYK	spleen tyrosine kinase
T	thymidylate
Tab	table
TAE	Tris-Acetate-EDTA

TAK	TGFβ-activated kinase
TCR	T-cell receptor
TGF	transforming growth factor
TH	tec homology
TK	tyrosine kinase
TLR	Toll like receptor
TNF	tumor necrosis factor
TRAF	TNF receptor associated factor
TRIS	Tris(hydroxymethyl)aminomethane
U	units
V	variable/ Volt
Vol	volume
W	Watt
WHO	World Health Organization
wt	wildtype
ZAP-70	Zeta-chain-associated protein kinase 70
α	alpha
β	beta
γ	gamma
δ	delta
ε	epsilon
ζ	zeta
θ	theta
κ	kappa

λ	lamda
µ	micro

3 Abstract

In 2010, a conditional mouse model with the patient-derived translocation t(5;9)(q33;q22) was published. This translocation was discovered in a subtype of lymphoma, the peripheral T-cell lymphoma-not otherwise specified (PTCL-NOS). The genetic event fuses the spleen tyrosine kinase (SYK) gene with the interleukin-2 inducible T-cell kinase (ITK) gene (Streubel *et al.*, 2006).

Pechloff *et al.* demonstrated that the fusion protein ITK-SYK leads to activation of T-cell receptor (TCR) signaling. It was shown that transgenic ITK-SYK mice developed a lymphoproliferative disease comparable to the human peripheral T-cell lymphoma (PTCL) phenotype. This included T-cell activation, clonal T-cell proliferation as well as T-cell infiltration of peripheral organs (Pechloff *et al.*, 2010). Mucosa associated lymphatic tissue 1 (MALT1) has been identified as an important protein in the canonical nuclear factor kappa-light-chain-enhancer of activated B-cells (NF-κB) pathway which is a key regulator of T-cell activation and proliferation (Oeckinghaus *et al.*, 2007). Gain-of-function mutations of MALT1 are described in B-cell lymphoma, and its caspase-like proteolytic domain has been identified as therapeutic target for MALT1 inhibitors.

To investigate the role of MALT1 in the downstream signaling cascade of ITK-SYK mediated lymphoma initiation, ITK-SYK^{CD4Cre} mice were crossed with MALT1 knockout mice. These newly created ITK-SYK^{CD4Cre}MALT1$^{-/-}$ mice lived significantly longer than ITK-SYK^{CD4Cre} mice. Histopathologically, in diseased ITK-SYK^{CD4Cre}MALT1$^{-/-}$ mice, T-cell infiltration was demonstrated in the lymph nodes only. *Ex vivo* analysis of T-cells from ITK-SYK^{CD4Cre}MALT1$^{-/-}$ mice indicated less proliferation and higher apoptosis rates. According to these results, MALT1 is acting downstream of ITK-SYK as important signaling protein in the initiation cascade of ITK-SYK mediated T-cell lymphoma. Further research is needed to evaluate whether MALT1 is also involved in tumor maintenance and if blockage of MALT1 paracaspase activity should be considered as a therapeutic approach in lymphoma with confirmed ITK-SYK translocation.

4 Introduction

4.1 T-Cell Lymphoma

The term lymphoma describes a heterogeneous group of neoplasia that derive from lymphocytes. They can be differentiated into Hodgkin and Non-Hodgkin lymphoma (NHL) (Longmore *et al.*, 2001). As summarized in the WHO GLOBOCAN report, the incidence of these tumors in Europe was approximately 150 000 in 2012; males were slightly more affected than females (Ferlay J, 2013).

In 2008, the World Health Organization (WHO) published an updated version of the ´Classification of neoplasms of the hematopoetic and lymphoid tissues´ (Swerdlow, 2008). This classification set a new standard in diagnosis and therapy of lymphoma regarding its morphology, immunophenotype, genetics, molecular background and clinical presentation. It groups the different hematopoietic and lymphoid neoplasm into five major categories: (i) Mature B-cell neoplasm, (ii) mature T-cell and Natural Killer (NK) cell neoplasm, (iii) Hodgkin Lymphoma, (iv) histocytic and dendritic cell neoplasm, and (v) posttransplantation lymphoproliferative disorders (Campo *et al.*, 2011).

The group of mature T-cell and Natural Killer cell neoplasm consists of 21 different diseases. PTCL-NOS is the most common subtype (International Peripheral T-Cell and Natural Killer/T-Cell Lymphoma Study: Pathology Findings and Clinical Outcomes, 2008). Overall, approximately 5-10 % of NHL are diagnosed as PTCL with the highest prevalence in Asia (Anderson *et al.*, 1998). Among those PTCL who are primarily located in the lymph node, angioimmunoblastic T-cell lymphoma (AILT) and anaplastic large cell lymphoma (ALCL) are well characterized by their specific molecular pattern. Both AILT and ALCL were classified as PTCL-NOS before they could be identified as specific subentities.

By contrast, PTCL-NOS is characterized as a nodal PTCL with no molecular marker or typical immunophenotypic pattern which is true for 30-50% of all

PTCL (Iqbal *et al.*, 2014). Thus, diagnosis is primarily a diagnosis by exclusion.

The prognosis of patients with PTCL-NOS remains poor. One possible reason for poor prognosis might stem from the fact that PTCL-NOS is not a homogenous tumor entity but is comprised of several subtypes. The usual first line therapy for PTCL is a chemotherapy scheme consisting of CHOP (Cyclophosphamid, Hydroxydaunorubicin, Vincristin, Prednisone). Recent studies suggest a survival advantage in younger patients if Etoposide is added (Beaven and Diehl, 2015). PTCL-NOS are known to be highly proliferative which results in good initial response rates to chemotherapy. However, five years after diagnosis, the median overall survival rate is approximately 32%, mainly because of relapse (Armitage, 2012).

Different studies have tested new approaches towards PTCL-NOS treatment including second and third generation regimes, radiotherapy and stem cell transplantation. However, large randomized prospective studies are missing and not every patient qualifies for stem cell transplantation, which is associated with a high risk of therapy-associated death (d'Amore *et al.*, 2015). This calls for new therapeutic options, especially for those patients who do not qualify for stem cell transplantation due to increased age and/or a reduced general condition. Currently conservative treatment options for PTCL-NOS remain unsatisfactory, therefore it is essential to define new subtypes of PTCL-NOS, study the underlying signaling pathways and identify possible therapeutic targets which might lead to more individual therapeutic strategies in the future.

4.2 T-Cell Biology

The understanding of physiological T-cell receptor signaling is fundamental to comprehend the mechanisms involved in T-cell lymphomagenesis. Blockage of key molecules in signaling cascades is a common pharmaceutical strategy for treatment of haematological malignancies. Therefore, the study of the exact mechanisms of T-cell receptor signaling is crucial to identify key molecules for intervention. However, so far effective clinical use of these mechanisms in

lymphoma therapy has only been proven for B-cell lymphoma This includes a new chemotherapy-free treatment approach offered by substances such as Idelalisib, approved since 2015 for Europe. This small molecule inhibitor specifically blocks phosphatidylinositol 3-kinase δ (PI3K δ), a key molecule in B-cell receptor signaling, and it has been shown to increase survival rates in low grade malignant B-cell lymphoma such as chronic lymphocytic B-cell leukemia. Comparable to this molecule is Ibrutinib, an inhibitor of Bruton's tyrosine kinase. Both substances are well tolerated and offer a good alternative to traditional chemotherapy regimes (Wiestner, 2015).

Similarly effective substances for the treatment of T-cell lymphoma are missing, although the experience from B-cell lymphoma therapy suggest that blockage of signaling pathways could be a strategic approach.

4.2.1 Proximal T-Cell Receptor Signaling

The TCR signaling cascade is initiated upon MHC:antigen detection. This results in the phosphorylation of the ITAMs by lymphocyte-specific protein tyrosine kinase (LCK) (attached to CD4/CD8) and the proto-oncogene tyrosine-protein kinase FYN (attached to CD3 and ζ chains). Both LCK and FYN are members of the sarcoma (Src) tyrosine kinase family. CD45 signaling is necessary for the maintenance of LCK and FYN activity. Phosphorylated ITAMs are then able to bind and activate the Zeta-chain-associated protein kinase 70 (ZAP-70) via its Src-homology 2 (SH2) domains. Activated ZAP-70 phosphorylates LAT and SH2 domain containing leukocyte protein of 76kDa (SLP-76), which leads to the recruitment of phospholipase C (PLC)-γ. PLC-γ phosphorylation and activation is accomplished by ITK. It hydrolyses phosphatidylinositol-4,5-bisphosphate (PIP_2) into diacylglycerol (DAG) and inositol (1,4,5)-trisphosphate ($IP_{3)}$. Both PLC-γ and ITK activation is supported by co-stimulatory signals from CD28 dependant PI3K activation which leads to the generation of phosphatidylinositol-3, phosphatidylinositol-4,5-bisphosphate 4,5-bisphosphate (PIP_3). PIP_3 is a lipid and serves as an adaptor to direct pro-

teins to the membrane, especially those with a pleckstrin homology (PH) protein domain, such as PLC-γ and ITK (Janeway, 2008).

As mentioned previously, DAG and IP_3 are generated by PLC-γ mediated cleavage of PIP_2. DAG recruits proteinkinase C (PKC) θ to the cell membrane. This is the start of the formation of the CBM (Caspase activation and recruitment domain (CARD)-containing membrane-associated guanylate kinase (MAGUK) protein 1 (CARMA1)/ B-cell-lymphoma 10 (BCL10)/ MALT1) complex which leads to NF-κB activation. Furthermore, DAG activates mitogen-activated protein kinases (MAPK) signaling pathways via rat sarcoma (RAS), which leads to the activation of the transcription factor activator protein-1 (AP-1). In parallel, IP_3 binds to IP_3 receptors in the endoplasmatic reticulum and induces a Ca^{2+}-dependant activation of calcineurin. This induces a signaling cascade which amounts in the activation of the transcription factor nuclear factor of activated T-cells (NFAT). All three transcription factors NF-κB, NFAT and AP-1 induce IL-2 production and hence contribute to cell activation and proliferation (Fig. 1) (Janeway, 2008).

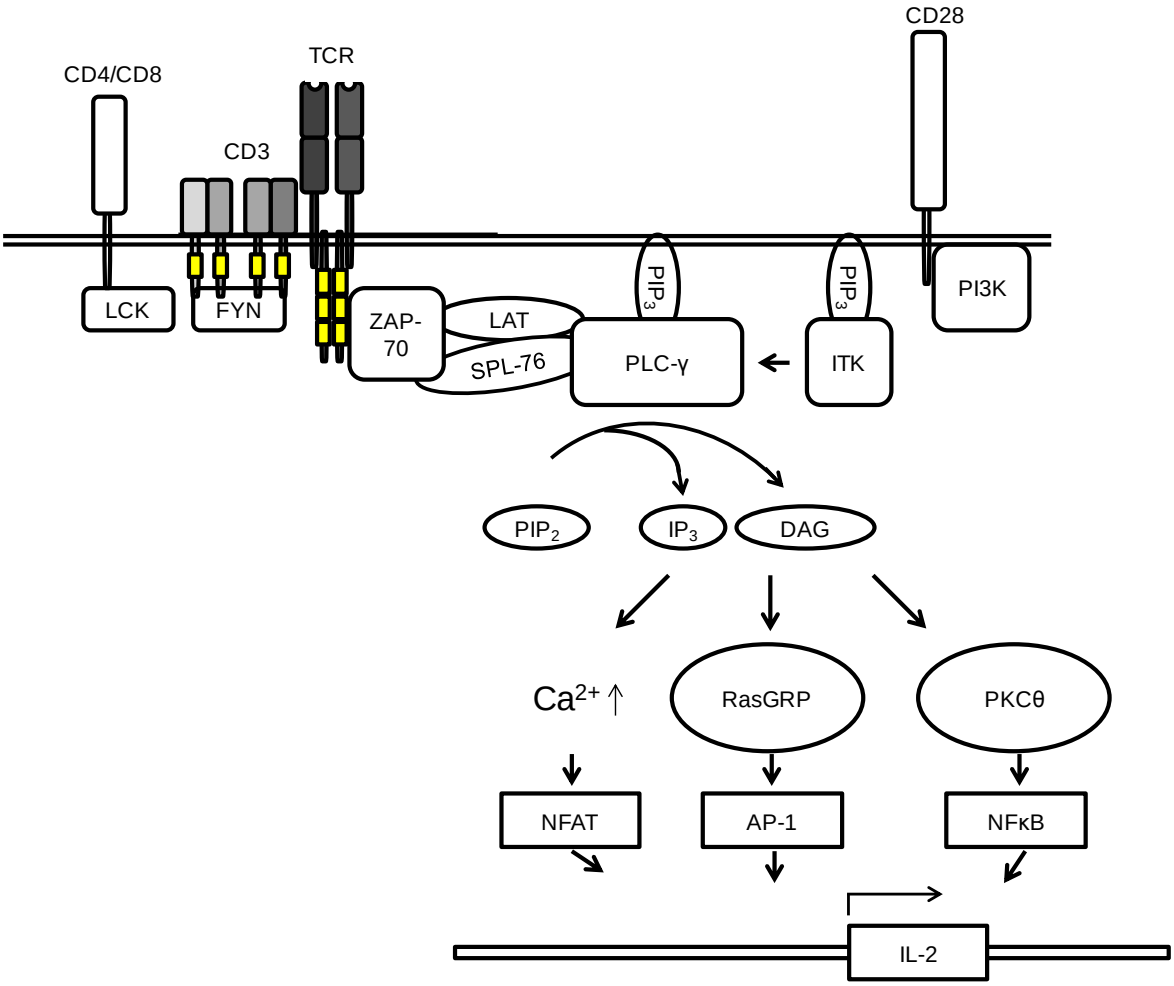

Fig. 1: Basic Scheme of TCR Signaling. *TCR-activation in combination of activation of the costimulatory molecule CD28 leads to the initiation of several pathways eventually resulting in the production of the key T-cell cytokine, IL-2 (modified from Janeway, 2008).*

4.2.2 The NF-κB Pathway

NF-κB was discovered in 1986 originally as a protein complex which was binding to the κ light chain enhancer in B-cells and as such acting as a transcription factor (Sen und Baltimore, 1986). Due to the high number of possible target genes (more than 150) which includes cytokines, chemokines, immune receptors, cell adhesion molecules, acute phase proteins, and regulators of apoptosis (Pahl, 1999), the NF-κB protein complex is one of the key factors involved in innate and adaptive immunity.

The family of NF-κB in mammalia comprises of five members: Related protein (Rel)A, RelB, c-Rel, p50 (precursor p105), and p52 (precursor p100) (Nabel and Verma 1993). All of them possess a rel homology domain which contains a nuclear localization sequence and is responsible for protein dimerization, interaction with Inhibitor of κB (IκB), as well as the ability to bind deoxyribonucleic acid (DNA), thus activating gene transcription (Ghosh *et al.*, 1998). RelB and p100 adopt an important role in the signaling cascade of the non-canonical NF-κB pathway which imparts with cell maturation, differentiation, and development of secondary lymphoid tissues (Dejardin, 2006). RelA and p50 are involved in the canonical pathway which is activated upon pro-inflammatory stimulation including the Toll-like receptor (TLR), the tumor necrosis factor (TNF) receptor and the B- and T-cell receptors (Li and Verma, 2002).

4.2.3 From CBM Complex Formation to NF-κB Activation

In 2001, Ruland *et al.* discovered that BCL10 knockout mice were prone to infections and that NF-kB signaling could not be engaged by TCR stimulation. Additionally, neither inhibitor of kappa B kinase (IKK) phosphorylation nor IκB degradation occurred suggesting that in the signaling cascade, BCL10 was located upstream of IKK (Ruland *et al.*, 2001). In the same year it was demonstrated that BCL10 was not directly binding to IKKγ but strongly connecting with MALT1 and that the formation of the BCL10/MALT1 complex was indispensable for TCR mediated NF-κB activation signaling (Lucas *et al.*, 2001). Furthermore, evidence was provided that CARMA1, a member of the MAGUK protein family, was linking PKC-θ with BCL10 and that CARMA1, BCL10 and MALT1 were forming a ternary complex in the cytosol (McAllister-Lucas *et al.*, 2011), hence called the CBM complex.

Upon CBM complex generation, BCL10 and MALT1 oligomerize, induce TNF receptor associated factor 6 (TRAF6) oligomerization and thus activate its ubiquitin ligase activity. This results in self-ubiquitination of TRAF6 and poly-ubiquitination of the regulatory subunit of IKK, IKKγ/ NF-kappa-B essential

modulator (NEMO). Ubiquitinated TRAF6 activates and triggers autophosphorylation of TGFβ activated kinase-1 (TAK1). Finally, phosphorylated TAK1 induces IKK complex activation by IKK β phosphorylation (Fig. 2).

IKK β phosphorylates IκB which forms a complex with RelA and p50. IκB contains ankyrin rich regions for NF-κB interaction and a signal responsive region which serves as phosphorylation site. Upon phosphorylation of IκB, which marks it for polyubiquitination and proteasomal degradation, NF-κB is released and being translocated into the nucleus where it acts as transcription factor. Among many other genes, NF-κB enhances transcription of the IκB gene thus self-regulating its activity by a regulatory feedback loop (Ghosh *et al.*, 1998) (Fig. 2).

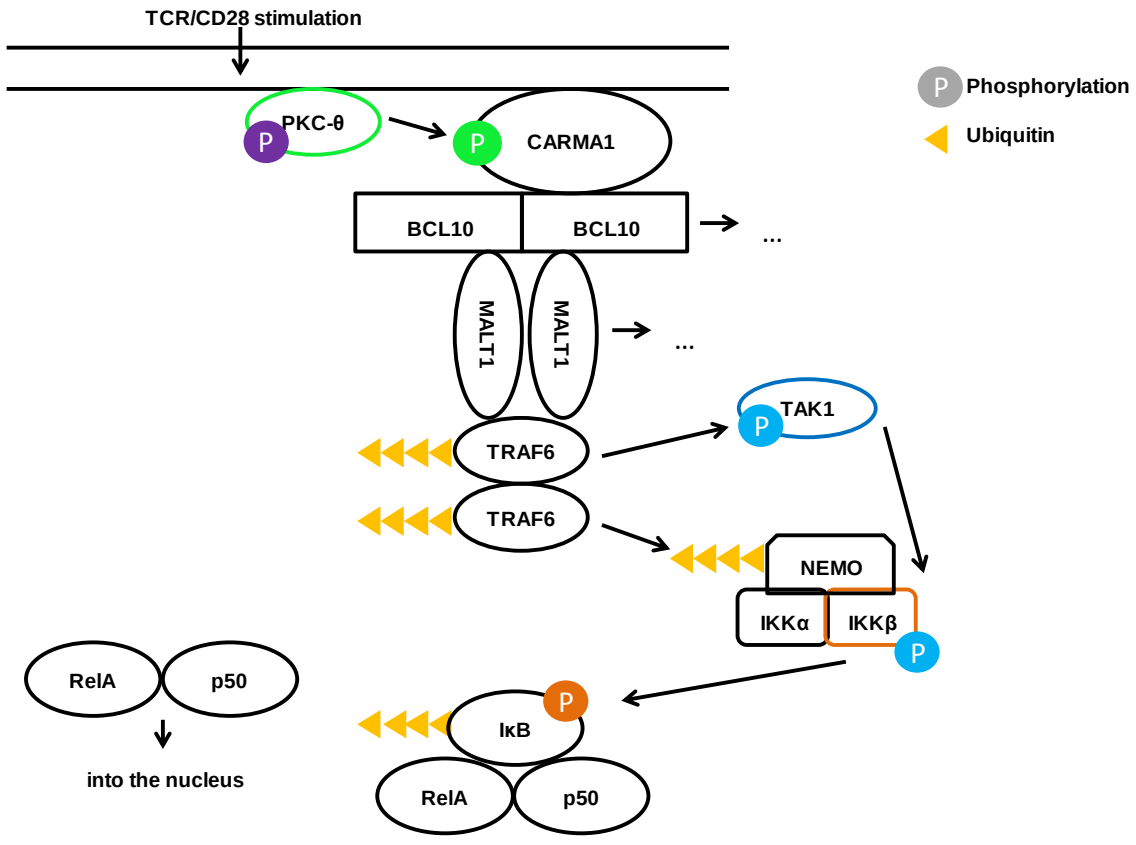

Fig. 2: Schematic Overview of NF-κB signaling upon TCR/CD28 Stimulation in T-cells. *The PKC θ dependant formation of the CARMA1/BCL10/MALT1 complex eventually initiates the release of RelA/p52 via IκB phosphorylation. In detail, BCL10/MALT1 oligomerization induces TRAF6 oligomerization which results in phosphorylation of TAK1. This allows the phosphorylation of IKK β and IκB which leads to NF-κB activation.*

4.2.4 MALT1 – Physiology and Role in Lymphoma

MALT1 is a paracaspase with scaffolding and proteolytic activity. It consists of an amino-terminal death domain, three immunoglobulin (Ig)-like protein-protein interaction domains, and a caspase-like proteolytic domain. (McAllister-Lucas *et al.*, 2011).

Fig. 3: Protein Structure of MALT1. *The amino-terminal death domain (DD) (function unknown) is followed by two Ig domains which mediate BCL10 interaction. The caspase-like (Casp-L) domain mediates cleavage activity and is responsible for cleavage of a variety of proteins which are involved in the NF-kB signaling pathway. The third Ig domain contains sites for mono- and polyubiquitination.*

MALT1-deficient mice present with immunodeficiency due to impaired immune responses upon immune receptor activation including the TCR, BCR and Fc receptors which are expressed on myeloid and mast cells (Ruland *et al.* 2003; Klemm *et al.* 2006). All of those immunoreceptors contain ITAM motives which activate MALT1 via PKC and CARD proteins such as CARMA1 (Matsumoto *et al.* 2005).

MALT1 as a scaffold recruits protein complexes for NF-κB activation. Via its proteolytic activity, negative NF-κB regulators are cleaved for signal enforcement. This includes A20 and RelB, which are cleaved by MALT1 paracaspase, leading to an extension of NF-κB response. In addition, autoprocessing of MALT1 results in NF-κB activation, probably due to NF-κB target gene expression (Baens *et al.* 2014).

Other known substrates of MALT1 paracaspase are a set of mitochondrial ribonucleic acid stability modulators. This includes Regnase1, an RNAse, and the Roquin-1 and -2 proteins which promote mRNA degradation. MALT1-dependant cleavage of these mRNA stability modulators reduces its levels in activated T-cells, resulting in stabilization of pro-inflammatory proteins such as IL-6 and IL-2 (Jaworski and Thome, 2016).

Deregulation of MALT1 activity with constitutive NF-κB signaling is a known underlying factor in lymphoma development. Since the paracaspase plays a key role in MALT1 dependant NF-κB signaling, blockage could be a potential strategy to treat lymphoproliferative diseases. Indeed, a variety of MALT1 inhibitors is available and currently in preclinical use, especially in the context of diffuse large B-cell lymphoma (DLBCL) (Fontan *et al.*, 2012).

The ITK-SYK protein was shown to activate antigen-independent proximal T-cell signaling, which is also necessary for NF-κB signaling activation. So far, MALT1 targeting in T-cell lymphoma is not described as an efficient treatment approach. In this thesis, the effects of MALT1 absence in a specific subtype of PTCL with proven t(5;9)(q33;q22) are demonstrated.

4.3 ITK-SYK t(5;9)(q33;q22) – Defining a New Subtype of PTCL

In 2006, the chromosomal translocation t(5;9)(q33;q22) was identified in five of 30 tissue samples derived from PTCL-NOS patients. On a molecular level, this translocation event results in the combination of protein domains of ITK and SYK (Streubel *et al.*, 2006) (Fig. 4).

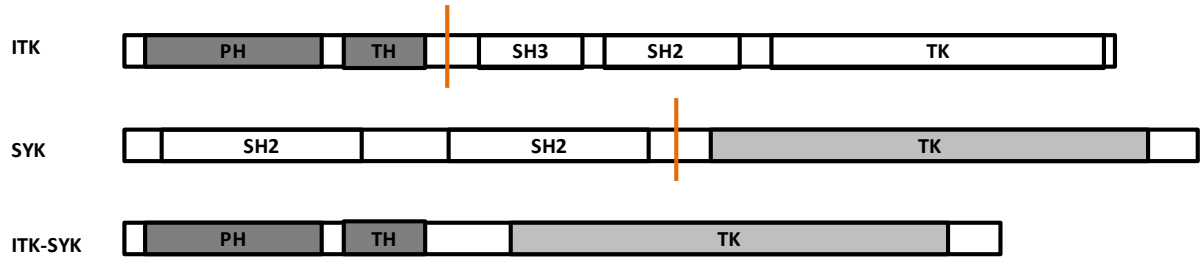

Fig. 4: Protein Structure of the Kinases ITK, SYK and Fused ITK-SYK. *The translocation event t(5;9)(q33;q22) leads to the expression of the fusion protein ITK-SYK. On the level of the domain structure, the pleckstrin homology (PH) domain and the proline-rich Tec homology (TH) domain of ITK are fused with tyrosine kinase (TK) domain of SYK (modified from Pechloff et al., 2010).*

The physiological function of ITK, a member of the Tec family kinases which is expressed in T-lymphocytes, consists of T-cell development in the thymus and

proximal TCR signaling, especially in CD4+ T-cells (Liao and Littman, 1995). Consistent with these findings, ITK interacts with PIP_3 via its PH domain. This leads to co-localization of ITK with the TCR complex which is required for PLC-γ cleavage. The adaptor proteins SLP-76 and LAT have been identified as further signaling partners of ITK, which emphasizes its role in proximal TCR signaling (Hirve *et al.*, 2012).

SYK, as well as ZAP-70, belong to the SYK family protein-tyrosine kinases. In B-cells, SYK is essential for B-cell development and B-cell receptor (BCR) signaling. Whereas ZAP-70 is responsible for well-defined events within the TCR signaling cascade, the role of SYK in T-cells is still unknown. Expression levels suggest a role in the double negative (DN) and double positive (DP) stage of T-cell development. Furthermore, SYK mediates phosphorylation of the immunoreceptor tyrosine-based activation motives (ITAMs) in the ζ chain of the TCR complex, which indicates a supportive role in TCR signaling (Sada *et al.*, 2001).

In 2010, Pechloff *et al.* described *in vitro* mechanisms of ITK-SYK driven PTCL. ITK-SYK was detected in the lipid rafts of T-cells and also induced phosphorylation of the adaptor molecules SLP76, LAT and of PLC-γ, the latter being a key molecule of TCR signaling. Furthermore, IL-2 production was enhanced and surface expression of CD69 as an early marker of T-cell proliferation was upregulated. These findings stated that ITK-SYK is acting as a constitutive antigen-*independent* stimulator of proximal TCR signaling events. Additionally, Pechloff *et al.* established a conditional transgenic ITK-SYK mouse model. Human ITK-SYK fusion cDNA together with an internal ribosomal entry site (IRES) enhanced green fluorescent protein (eGFP) sequence, preceded by a loxP-flanked transcriptional and translational STOP cassette, was inserted into the ubiquitously expressed Rosa 26 locus. The resulting mice were crossed with transgenic CD4Cre animals, creating ITK-SYK^{CD4Cre} mice, thus enabling a setting where ITK-SYK expression was restricted to the T-cells. These mice developed a lymphoproliferative disease with features similar to human PTCL (Pechloff *et al.*, 2010).

Constitutive NF-κB signaling can be detected in a variety of lymphoid malignancies, especially in B-cell lymphoma but also in T-cell lymphoma (Courtois und Gilmore, 2006). NF-κB signaling is required for T-cell activation and proliferation. This suggested that ITK-SYK activity might influence key proteins of the NF-κB signaling pathway.

Experiments with ITK-SYK transfected Jurkat T-cells revealed that treatment with MALT1 inhibitors led to significantly reduced IL-2 levels compared to untreated ITK-SYK Jurkat T-cells (Holch, unpublished data). This data suggested that MALT1 was involved in ITK-SYK signaling.

Thus, the published ITK-SYK mouse model was used in this thesis to investigate the role of MALT1 in ITK-SYK driven lymphomagenesis with a specific emphasis on the disease outcome. As peripheral T-cell lymphoma are characterized as a CD4+ T-cell dominant entity (Savage, 2005), ITK-SYK^{CD4Cre} mice which had been created and investigated by Pechloff *et al.* and MALT1$^{-/-}$ mice were used to create ITK-SYK^{CD4Cre}MALT1$^{-/-}$ mice. These ITK-SYK^{CD4Cre}MALT1$^{-/-}$ mice possessed the human ITK-SYK protein but were MALT1 deficient to enable the investigation of MALT1 function in ITK-SYK downstream signaling.

5 Material and Methods

5.1 Material

5.1.1 Technical Devices

The following chart lists those technical device which have had an important role in data acquisition and analysis. Apart from these instruments, standard lab equipment was used.

Technical Device	Company
Benchtop centrifuge for samples more than (>) 2 milli(ml)litre (l): Rotina 380R	Hettich
Benchtop centrifuge for samples less than (<) 2 ml: Centrifuge 5417R	Eppendorf
Fluorescence-activated cell sorting (FACS) Canto II Flow Cytometer	BD Bioscience
Light microscope: DMIL light-emitting diode (LED)	DMIL LED, Leica
Polymerase Chain Reaction *(PCR)* –Thermocycler	Bioline

Table (Tab.) 1: Technical Devices.

5.1.2 Reagents

Substance	Company
5-Mercaptoethanol 50 milliMolar (mM)	Gibco
Acetic acid	Roth
Agarose	Peqlab
Aqua ad iniectabilia	Braun
Aqua destillata (dest.)	Braun
DNA Ladder 100 base pairs	Fermentas
DNA Loading Dye 6x	Fermentas

Substance	Company
Deoxyribonucleotide triphosphates (dNTP) mix 2.5mM each	Bioline
Ethydiumbromide	Applicam
Ethylenediaminetetraacetic acid (EDTA)	Roth
Fetal Calf Serum (FCS)	Gibco
Glutamine 200mM	Gibco
Isofluran	Abbott Animal Health Care
Paraformaldehyde 10%	J.T. Baker
Penicillin (10000 Units (U)/ml) /Streptomycin (10000 micro(µ)gram(g)/ml)	Gibco
Phire Polymerase Hot Start	Thermo Scientific
Phosphate buffered saline (PBS) 10x	Gibco
Proteinase K	Sigma
Tris(hydroxymethyl)aminomethane (TRIS)	Roth
Trypan blue 0.4%	Gibco

Tab. 2: Reagents.

5.1.3 Standard Solutions, Cell Media and Buffers

Solution/Medium/Buffer	Composition/ *Company*
Apoptose Binding Buffer	*eBioscience*
Cell Proliferation Dye (CPD) labeling medium	10% FCS 1 Volume (Vol)-% Glutamin 1 Vol-% Penicillin/Streptomycin 0.1 Vol-% 5-Mercaptoethanol (50mM) in RPMI Medium

Solution/Medium/Buffer	Composition/ *Company*
Digestion solution master mix	200 µl Nuclei Lysis Solution 50 µl 0,5M EDTA (ph 8,0) 20 µl Proteinase K 20 mg/ml 5 µl Ribonuclotid Acid (RNA)se Solution 4mg/ml (all from Wizard SV Genomic DNA Purification Kit) 20 µl Proteinase K 20 mg/ml
Easycoll separating solution (ESS)	*Biochrom*
FACS buffer	Aqua dest. + 3% FCS
Mouse Cell Medium	3% FCS 1 Vol-% Glutamine (200mM) 1 Vol-% Penicillin/Streptomycin (100U/ml) 0.1 Vol-% 5-Mercaptoethanol (50mM) in RPMI 1640 Gibco®
Percoll solution	40%: PBS with 40% ESS 80%: PBS with 80% ESS
Red Blood Cell (RBC)-Lysis buffer	*eBioscience*
RPMI Medium	*Gibco*
Tris-acetate-EDTA (TAE) Buffer	0,4 M TRIS 1.1% Acetic Acid 2.0% 0,5 M EDTA (pH 8) in Aqua dest.
Washing Buffer	RPMI medium *(Gibco)* + 1% FCS

Tab. 3: Standard Solutions, Cell Media and Buffers.

5.1.4 Employed Antibodies

Antibodies were used to identify extracellular surface markers in different experimental settings.

Fluorochrome-conjugated Antibodies

Antibodies conjugated to fluorochromes were used for flow cytometric analysis. All antibodies were bought from eBioscience and conjugated to one of the following fluorochromes: Phycoerythrin (Pe), Phycoerythrin cyanin 5 (Pe-Cy5), Phycoerythrin cyanin 7 (Pe-Cy7), Allophycocyanin (APC), Alexa Fluor (AF).

Antibody	Dilution	Marker for
Anti-mouse B220	1:250	B-cells
Anti-mouse CD4	1:400	CD4+ T-cells
Anti-mouse CD8a	1:400	CD8+ T-cells
Anti-mouse CD11b	1:1000	Myeloid cells
Anti-mouse CD25	1:200	Lymphocyte activation
Anti-mouse CD44	1:400	Lymphocyte activation
Anti-mouse CD62L	1:200	Lymphocyte activation
Anti-mouse CD69	1:200	Lymphocyte activation
Anti-mouse F4/80	1:330	Macrophages
Anti-mouse Gr-1	1:1000	Granulocytes
Anti-mouse TCRβ	1:400	T-cells

Tab. 4: Fluorochrome-conjugated Antibodies.

Unconjugated Antibodies

Unconjugated antibodies were used in several experimental settings to identify specific epitopes.

Antibody	Dilution	Marker for	Company
Anti-mouse CD11b	1:150	Myeloid cells	ebioscience
Anti-mouse CD16/CD32	1:200	Unspecific IgG detection	ebioscience

Antibody	Dilution	Marker for	Company
Rabbit Anti-syrian Hamster IgG (H+L)	1:240	heavy and light chains of the IgG molecule	Jackson Immuno Research
Anti-mouse CD3	1:100	T-cell receptor subunit	eBioscience
Anti-mouse CD28	1:125	Costimulatory receptor for TCR signaling	eBioscience

Tab. 5: Unconjugated Antibodies.

5.1.5 Beads

Magnetic beads	Company
Dynabeads® mouse pan B	Invitrogen
Dynabeads® sheep anti rat IgG	Invitrogen

Tab. 6: Magnetic Beads.

5.1.6 Dyes for Cellular Proteins/DNA

Dye	Company
Annexin V	eBioscience
CPD eFluor®670	eBioscience
7-amino-actinomycin D (7AAD)	eBiosience

Tab. 7: Dyes for Cellular Proteins/DNA.

5.1.7 Primers

The following primers were used for PCR analysis of mouse tail genomic DNA. Primers were obtained from Sigma-Aldrich:

Primer	5`-3` sequence
CD4Cre_fwd	ACCAGCCAGCTATCAACTCG
CD4Cre_rev	TTACATTGGTCCAGCCACC
ITK-SYK_fwd	GATGGATGGGAAGTGGAGGTG
ITK-SYK_rev	GGACCAAGTTCTGCCATCTC
MALT1_com	CTGCTGCTGACATGCTACAATATGCTG
MALT1_neo	GGGTGGGATTAGATAAATGCCTGCTC
MALT1_wt	ACTTTCATCTTGCCAGCACTCTTTCTTA

Tab. 8: Employed Primers.

5.2 Methods

5.2.1 Mouse Husbandry

All animals were kept in a specific pathogen free environment to enable standardized conditions. Efforts were met to meet the requirements of the Animal Welfare Act. Animals were sacrified upon signs of disease which included lethargy, open wounds, inflammatory signs, paralysis, horrent coat, hunchy posture or severe weight loss.

5.2.2 Breeding Strategy

As peripheral T-cell lymphoma are characterized as a CD4+ T-cell dominant entity (Savage, 2005), ITK-SYK mice as created and investigated by Pechloff *et al*. (Fig. 5) were crossed with animals which expressed the Cre recombinase under the control of the CD4 promoter (referred to as CD4Cre mice) (Lee *et al.*, 2001). Additionally, both ITK-SYK mice and CD4Cre mice had a knockout background of MALT1 (Ruland *et al.*, 2003) to create ITK-SYK^{CD4Cre}MALT1$^{-/-}$ mice.

Fig. 5: Schematic Representation of the ITK-SYK Vector. *The stop cassette is floxed to allow itk-syk activation in specific cell types by Cre recombinase (modified from Pechloff et al., 2010).*

To compare ITK-SYK^{CD4Cre}MALT1$^{-/-}$ with ITK-SYK^{CD4Cre} mice in parallel, new ITK-SYK^{CD4Cre} mice were analyzed additionally. All mice used were of mixed C57BL/6 and 129P2/OlaHsd genetic background.

5.2.3 Mouse Genotyping

PCR is a well-established method for DNA multiplication and was used for mouse genotyping. Gene sequences were amplified from the following targets: ITK-SYK, Cre recombinase and MALT1. MALT1 required two PCRs to test for homo- or heterozygosity.

Genomic DNA was generated from mouse tails which were taken from mice anaesthetised with Isofluran. DNA isolation was carried out according to the Wizard® SV Genomic DNA Purification Kit (Promega) instructions. The general PCR setup was composed of 10 nano(n)g DNA template, dNTPs (Bioline), primers (Sigma), Phire Polymerase (Thermo Scientific) and 5x Phire Reaction Buffer (Thermo Scientific) in different compositions. All steps of the reaction cascade (denaturation, annealing, elongation) were carried out by a PCR thermocycler (Biorad).The following tables give information on the composition of the PCR master mix as well as duration and temperature of the individual PCR steps:

PCR	Composition	Profile
Malt1 wildtype	2 µl template 5 µl reaction buffer 2 µl dNTPs	Initialization: 2', 98°C 35 cycles: Denaturation: 30', 98°C

	1 µl Malt1_wt primer	Annealing: 1', 62°C
	1 µl Malt1_com primer	Elongation: 1', 72°C
	0.2 µl Phire Polymerase	--
	13.8 µl H_2O	Final Elongation: 1', 72°C
Malt1 neo	2 µl template	Initialization: 2', 98°C
	5 µl reaction buffer	35 cycles:
	2 µl dNTPs	Denaturation: 30', 98°C
	1 µl Malt1_neo primer	Annealing: 1', 62°C
	1 µl Malt1_com primer	Elongation: 1', 72°C
	0.2 µl Phire Polymerase	--
	13.8 µl H_2O	Final Elongation: 1', 72°C
Cre	2 µl template	Initialization: 3', 98°C
	5 µl reaction buffer	30 cycles:
	2 µl dNTPs	Denaturation: 45'', 98°C
	0.3 µl CD4Cre_fwd primer	Annealing: 20'', 55°C
	0.3 µl CD4Cre_rev primer	Elongation: 10'', 72°C
	0.2 µl Phire Polymerase	--
	15.2 µl H_2O	Final Elongation: 1', 72°C
itk-syk	2 µl template	Initialization: 2', 98°C
	5 µl reaction buffer	35 cycles:
	2 µl dNTPs	Denaturation: 1', 98°C
	0.5 µl itk-syk_fwd primer	Annealing: 30'', 62°C
	0.5 µl itk-syk_rev primer	Elongation: 30'', 72°C
	0.2 µl Phire Polymerase	--
	16.2 µl H_2O	Final Elongation: 1', 72°C

Tab. 9: PCR used for Amplifying Murine DNA Sequences.

PCR DNA products were died with methylen blue, loaded onto a gel (200 ml TAE buffer with 2 g agarose) and run for 20 minutes (4 mAmpere (A), 120 mV, 300 W).

5.2.4 Lymphocyte Purification

T-cell purification of spleen and lymph nodes for proliferation and apoptosis assays was based on magnetic bead isolation whereas lymphocytes from liver, kidney and lung for FACS analysis were purified by density gradient centrifugation.

5.2.4.1 Magnetic Bead Purification

Principle: Myeloid cells were labelled with a CD11b antibody and attached to antibody-conjugated magnetic beads (*Dynabeads® sheep anti-rat IgG).* B-cells were attached to *Dynabeads® Pan B* which detect B220 which is expressed on the membrane throughout all developmental stages of B-cell maturation. Magnetically labelled cells were then put into a magnetic field. T-cells remained in the supernatant whereas non T-cells were magnetically directed to the wall of the tube (Neurauter *et al.*,2008).

Protocol: Spleen and lymph nodes were harvested and mashed. 2 ml of RBC-Lysis buffer were added followed by an incubation time of 5 minutes. Mouse Cell Medium was used to stop the osmotic process. The cell suspension was centrifuged at 350 rpm at RT for 5 minutes. The pellet was then resuspended in 3 ml of Washing Buffer. 20 µl of anti-mouse CD11b antibody (eBioscience) were added and the suspension was then incubated for 20 minutes at 10 degrees rotating. Afterwards, cells were washed twice with 10 ml washing buffer and finally resuspended in another 7 ml of washing buffer.

The bead master mix consisted of PanB beads (Invitrogen) (300 µl/mouse) and sheep anti rat IgG beads (Invitrogen) (200 µl/mouse). Beads were washed twice and then put on ice until the cells were ready for further processing. 500 µl of resuspended beads were added to the cell suspension and incubated for 30 minutes at 4 °C, rotating. The falcon was then put into the magnetic tube holder and the supernatant containing the T-cells was taken away. This step was carried out twice to ensure the maximum possible T-cell collection. T-cells were then centrifuged for 5 minutes at 350 rpm and resuspended in RPMI-Medium. Cells were stained with stain D (see table 14) to investigate the purity

of the T-cell suspension. An average of 90% T-cell purity could be achieved in the suspension from the control mice. Suspensions from ITK-SYK transgene expressing mice presented with 70% T-cell purity in average

5.2.4.2 Percoll Density Gradient Centrifugation

Principle: Solutions with different concentrations of colloidal silica particles coated with polyvinylpyrrolidone (PVP) have different densities. Centrifugation can then be used to isolate cell fractions between layers of different densities (Pertoft *et al.*, 1978).

Protocol: Liver, kidney and lung were harvested and mashed. 5 ml of RBC-Lysis buffer was added followed by an incubation time of 5 minutes. Mouse Cell medium was used to stop the osmotic process. Percoll solution (Biochrome) was diluted with PBS to a concentration of 40 and 80%, respectively. 6 ml were used for each sample. The dilution which contained 40% of Percoll solution was mixed with the cell pellet and then carefully underlaied by the 80% Percoll solution. After centrifugation (2400 rpm, 20 minutes, RT) a cloudy layer of lymphocytes appeared between the two Percoll solutions. The upper layer was extracted and the lymphocyte layer was pipetted into a new tube. The cells were stained according to chapter 5.1.4.

5.2.5 Flow Cytometry

Principle: Flow cytometry is a means to identify extracellular surface markers as well as intracellular cell components. Fluorochome-conjugated antibodies are applied to the cells of interest and bind to their specific antigen. Via laser technique, a flow cytometer can then analyze the cellular stimulated emission spectrum and provide information about the quantity of different cell markers.

Protocol (Solid Organs): Spleen, lymph nodes, liver, kidney, lung and bone marrow were harvested from mice. The organs were mashed and the cell suspensions were treated with RBC-Lysis buffer. Lymphocytes from liver, kidney and lung were isolated by Percoll gradient centrifugation according to chapter 5.2.5.2, whereas spleen, lymph node, thymus and bone marrow suspensions

were directly used for cell counting. Subsequently, cells were pretreated with anti-mouse CD16/CD32 antibody (diluted 1:200) to prevent unspecific binding of immunglobulins to F_c receptors.

The following stains were used:

Stain	Detected epitopes
A	B220, CD4, CD8, CD11b, TCRβ
B	CD4, CD8, CD44, CD62L
C	CD4, CD8, CD25, CD69
D	B220, CD11b, TCRβ

Tab. 10: Staining Compositions.

After an incubation time of 20 minutes, cells were washed with FACS buffer and then analyzed by a FACS Canto II flow cytometer (BD Bioscience).

Protocol (Blood): To monitor the percentage of lymphocytes which expressed eGFP in the blood, blood samples from mice were taken monthly. By puncturing the submandibular vein with a lancet (Golde *et al.*, 2005) approximately 0.3 ml of blood was obtained which was sufficient for FACS analysis. Blood samples were collected in tubes, coated with EDTA to stop coagulation and were processed within one hour (h) prior to acquisition.

Blood samples were incubated with 2 ml of RBC-Lysis buffer for 5 minutes (min) at room temperature (RT) to remove the erythrocytes. Lysis was stopped with FACS buffer and the samples were centrifuged at 4 degree Celsius (°C) and 350 rounds per minute (rpm) for 5 min. To improve sample purity, this step was repeated with another 1 ml of RBC-Lysis buffer. Afterwards, cells were stained with 0.5 µl of anti-mouse CD16/CD32 to block unspecific binding of antibodies. The samples were stained with the following fluorochrome-conjugated antibodies: CD11b, TCRβ, CD4, CD8 and B220, with concentrations according to table 4.

Staining was performed at 4 °C for 15 minutes. Each sample was washed with 5 ml of FACS buffer and centrifuged at 4 °C, 350 rpm for 5 minutes. Sample acquisition was done on a FACS Canto II flow cytometer.

Data of flow cytometric analysis was investigated by FlowJo software. Different gating strategies were used depending on the experimental settings.

5.2.6 Stimulation Experiments

Principle: CPD is a fluorescent which binds to primary amines of cellular proteins. Cell division leads to the equal distribution of the dye into the daughter cells. Its fluorescence intensity can be measured by Flow Cytometry. The intensity decreases after every cell division and this principle can be used to visualize different T-cell populations. CPD-labeled T-cells were used to analyze proliferation rates upon CD3/CD28 stimulation.

Protocol: Purified T-cells were washed twice with PBS to remove any traces of serum. Cells were resuspended at 2x the desired final concentration in PBS as labeling induced severe cell loss. While vortexing, 10 µM of CPD eFluor® 670 (eBioscience) were mixed 1:1 with the cell suspension. After an incubation step for 10 minutes at RT in darkness, labeling was stopped by adding the CPD labeling medium and cells were incubated on ice for 5 minutes. Cells were then washed three times with CPD labeling medium. Prior to the distribution of CPD-labeled T-cells into 96 well plates, the wells were coated with rabbit anti-syrian hamster (Jackson ImmunoResearch) (10 µg/ml) for at least 10 hours at 4 °C.

For each genotype, $1x10^5$ CPD-labeled T-cells were distributed into 21 wells each with 5% Mouse Cell Medium. 5 wells were used as unstimulated controls at 0 h, 24 h, 48 h, 72 h and 96 h. Additionally, cells were stimulated with α-CD3 antibody (5 µg/ml), α-CD3 antibody (5 ng/ml), α-CD3/CD28 antibody (5 µg/ml and 2 µg/ml) and α-CD3/CD28 antibody (5 ng/ml and 2 µg/ml) for 24 h, 48 h, 72 h and 96 h. Both CD3 and CD28 were bought from eBioscience. For final FACS-analysis, T-cells were harvested from the wells and stained with extracellular fluorescent antibodies directed against the following epitopes according to table 4: TCRβ, CD4 and CD8. Analysis revealed CD3/CD28 (5 ng/ml and 2 µg/ml) as the optimal concentration for analysis of cell proliferation.

5.2.7 Apoptosis Experiments

Principle: Annexin V binds to phosphatidylserine which physiologically is located on the inner leaflet of the plasma membrane. During early apoptosis, phosphatidylserine is translocated to the outer cellular membrane. Fluorochrome labeled Annexin V then binds to phosphatidylserine which can be detected by flow cytometric analysis (Koopman *et al.*, 1994). 7AAD is a fluorescent which interacts with DNA by intercalation and is a marker of late apoptosis (Rabinovitch *et al.*, 1986). Both substances were used to monitor apoptosis in all genotypes of interest.

Protocol: Per genotype, $5x10^5$ purified T-cells were distributed into 5 wells of a 96 well plate, each with 5% FCS Mouse Cell Medium. Cells were harvested after 0 h, 24 h, 36 h, 72 h and 96 h and washed once with FACS buffer prior to staining with antibodies directed against the epitopes of CD16/CD32, CD4, CD8 and TCRβ according to section 5.1.4. Afterwards, cells were washed with FACS buffer, followed by a washing step with PBS and a final washing step with Annexin V binding buffer (eBioscience) according to the manufacturers protocol. 5 µl of Annexin V- APC were added to 100 µl of cell suspension and incubated in the dark for 15 minutes at RT. Cells were then washed once with the Annexin V binding buffer. Subsequently, 4 µl of 7AAD (eBioscience) were added and the sample was analyzed on a FACS Canto II flow cytometer.

5.2.8 Histologies

Organs (spleen, lymph node, bone marrow, liver, kidney, lung, conchae) were gathered from mice and fixed at 4% formaldehyde for 12 h. Further steps included dehydration, paraffin wax infiltration, embedding, microtome sectioning and staining. Stains of interest were the Haematoxylin and Eosin stain for tissue overview, MIB1 (antibody directed against Ki-67 as a marker for apotosis) and the anti-CD3 antibody for T-cell detection. All steps from dehydration onwards were performed by technicians of the Department of Pathology at the Technical University of Munich.

5.2.9 Statistical Analysis

The unpaired two-tailed student's t test was used to test for significant differences between two *independent* data sets. It was assumed that all values followed a Gaussian distribution. The null hypothesis was defined by the assumption that the means of two normally distributed data sets were equal. If the p-value exceeded 0.05, the null hypothesis was declared true. Smaller or equal values indicated a significant difference between the data sets.

The following symbols were used to describe significance:

*	$p \leq 0.05$
**	$p \leq 0.01$
***	$p \leq 0.001$

The unpaired student's t test was conducted by the GraphPad Prism Software.

5.2.10 Software

The following software was applied to perform data analysis:

Prism (GraphPad, Version 5)
Excel (Microsoft, 2007)
FlowJo (Tree Star Inc., Version 8.8.7)

6 Results

To investigate the role of MALT1 in ITK-SYK mediated T-cell lymphomagenesis, ITK-SYK^{CD4Cre}MALT1$^{-/-}$ mice were analysed and compared to ITK-SYK^{CD4Cre} littermate mice. Young mice at the age of 4-6 weeks without symptoms were sacrificed to generate data on early disease characteristics. Older mice which had to be sacrificed due to severe disease symptoms are hence called deceased mice.

6.1 Clinical Characteristics

6.1.1 MALT1 Deficiency in ITK-SYK^{CD4Cre} Mice Results in Prolonged Survival and Decreasing Tumor Cell Load in the Peripheral Blood

To see whether MALT1 absence effects ITK-SYK mediated lymphomagenesis, longterm survival observations of ITK-SYK^{CD4Cre} (number of animals tested (n) =11) and ITK-SYK^{CD4Cre}MALT1$^{-/-}$ (n=22) mice were initiated. Additionally, the percentages of eGFP+ T-cells in the blood as a marker for peripheral tumor cell load were monitored monthly via flow cytometry. Finally, animals of both cohorts were sacrificed according to predefined endpoints, including lethargy, open wounds, inflammatory signs, paralysis, horrent coat, hunchy posture or severe weight loss.

The analysis of the Kaplan-Meier curve (Fig. 6) revealed that ITK-SYK^{CD4Cre} animals reached a mean survival of 24 weeks. Clinically, these mice presented with a chronic decline of health including lethargy, hunched postures and/or paralysis of the hind limbs. On contrary, ITK-SYK^{CD4Cre}MALT1$^{-/-}$ animals reached a mean survival of 40 weeks which exceeded the mean survival of ITK-SYK^{CD4Cre} mice by 16 weeks. Four ITK-SYK^{CD4Cre}MALT1$^{-/-}$ animals, which corresponds to 18%, even survived more than 52 weeks. ITK-SYK^{CD4Cre}MALT1$^{-/-}$ mice did not show a slow deterioration of health but presented with acute symptoms including tachypnea, shivering and apathia appearing within hours. In combination with the underlying immunodeficiency due

to the MALT1 knockout background, these symptoms were interpreted as sepsis.

Monitoring the frequency of eGFP+ T-cells in the blood as a marker for peripheral tumor cell load was performed monthly. As described by Pechloff *et al.*, ITK-SYK^{CD4Cre} mice showed an expansion of eGFP+ lymphocytes in the blood alongside disease progression (Pechloff *et al.*, 2010) (Fig. 7 A). T-cells from ITK-SYK^{CD4Cre}MALT1$^{-/-}$ mice behaved differently and could be divided into two groups. Both groups started with high levels of eGFP+ lymphocytes in the blood. The first group (62%) exhibited a constant percental decline of eGFP+ lymphocytes whereas the second group (38%) remained at high levels (Fig. 7 B). This difference correlated with the survival time of the mice. Mice from group 1 had a mean survival time of 45.0 weeks, whereas mice from group 2 reached a mean survival of 32.8 weeks of age.

Data obtained from survival curves and blood samplings indicated an important function of MALT1 in ITK-SYK mediated lymphomagenesis. MALT1 deficient ITK-SYK^{CD4Cre} mice lived significantly longer than ITK-SYK^{CD4Cre} mice alongside with a continuous decline of lymphoma cells in the blood in the majority of analysed MALT1 deficient ITK-SYK^{CD4Cre} mice.

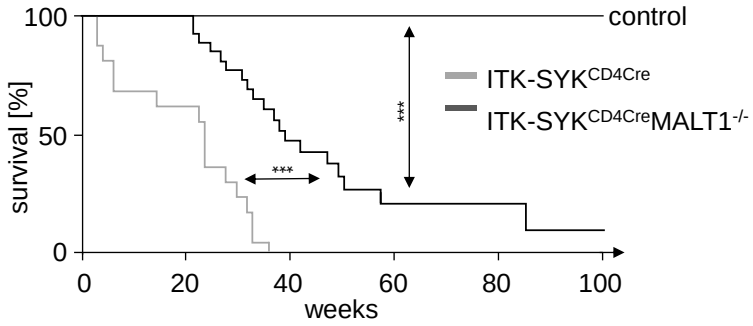

Fig. 6: Survival Curves. *Data was acquired from n = 11 mice with ITK-SYK^{CD4Cre} genotype and n = 22 mice with ITK-SYK^{CD4Cre}MALT1$^{-/-}$ genotype. The unpaired two-tailed Student's t test was used to analyze statistical significance (*** p ≤ 0.001). Controls (n=10) were defined as MALT1$^{-/-}$, MALT1$^{-/-}$ITK-SYK or MALT1$^{-/-}$CD4Cre mice.*

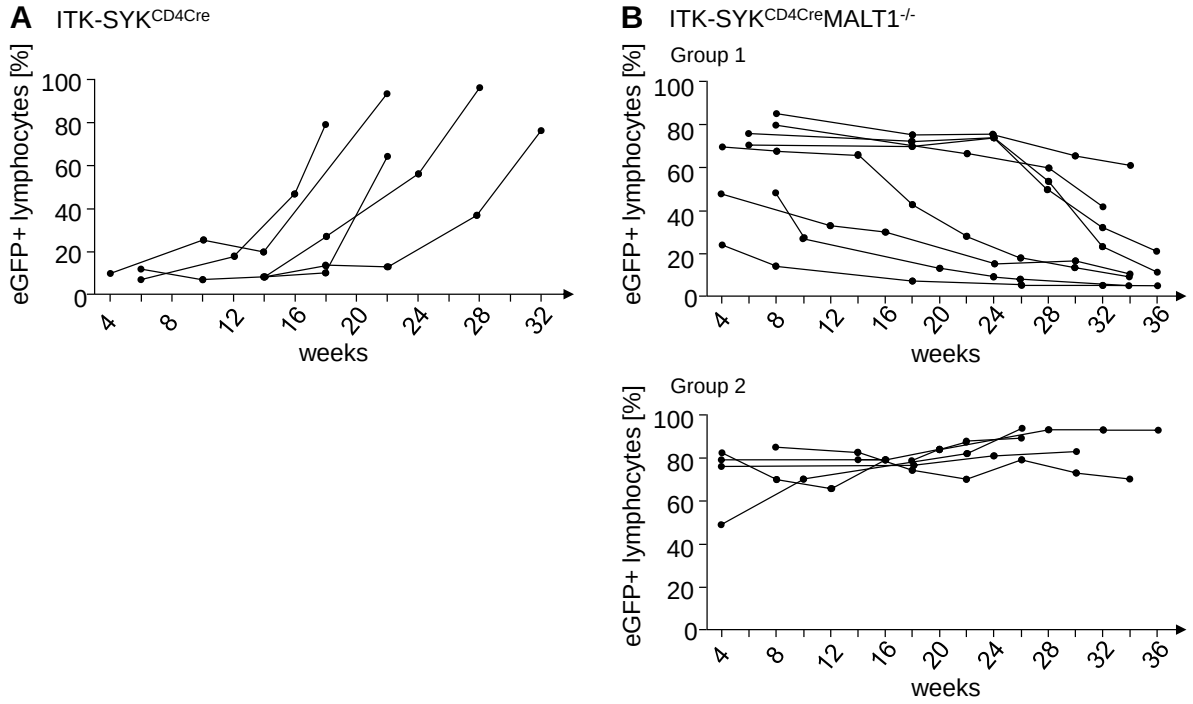

Fig. 7: Frequencies of eGFP+ Lymphocytes in the Blood over Time. *Peripheral blood samples were taken monthly from the submandibular vein. eGFP frequencies were measured by flow cytometry.* ***A*** *Development of the frequencies of eGFP+ lymphocytes over time in ITK-SYK^{CD4Cre} mice (n=5).* ***B*** *Development of the frequencies of eGFP+ lymphocytes over time in ITK-SYK^{CD4Cre}MALT1$^{-/-}$ mice identifies two distinct subgroups (n=8 (1), n=5 (2)).*

6.1.2 Deceased MALT1 Deficient ITK-SYK^{CD4Cre} Mice Present with Splenomegaly but Lymph Node Size Decreases over Time

The size of spleen and lymph nodes is a well-established indicator for disease stage in lymphoproliferative diseases. To see whether prolonged survival of MALT1 deficient ITK-SYK^{CD4Cre} mice was reflected in macroscopic features, spleen/mouse weight ratios and lymph node size of both ITK-SYK genotypes were measured and compared.

ITK-SYK^{CD4Cre} mice were introduced as a mouse model for PTCL-NOS with observed splenomegaly (Pechloff *et al.*, 2010). The same was shown for the majority of MALT1 deficient ITK-SYK^{CD4Cre} mice (Fig. 8 A). However, a small group of three out of 12 animals displayed spleen/mouse weight ratios comparable to their corresponding controls (Fig. 8 B).

In accord with a lymphoproliferative disease, lymph node size of ITK-SYK^{CD4Cre} mice increased over time (Pechloff *et al.*, 2010). In contrast, young MALT1 deficient ITK-SYK^{CD4Cre} mice presented with enlarged lymph nodes which decreased in size over time and were not seen in deceased ITK-SYK^{CD4Cre}MALT1$^{-/-}$ mice anymore (Fig. 8 C).

Although both ITK-SYK genotypes presented with splenomegaly, a vice versa scenario in lymph node size development was detected. This, together with findings from blood analysis, hinted towards a MALT1 depending mechanism in early T-cell development on a genetic ITK-SYK background.

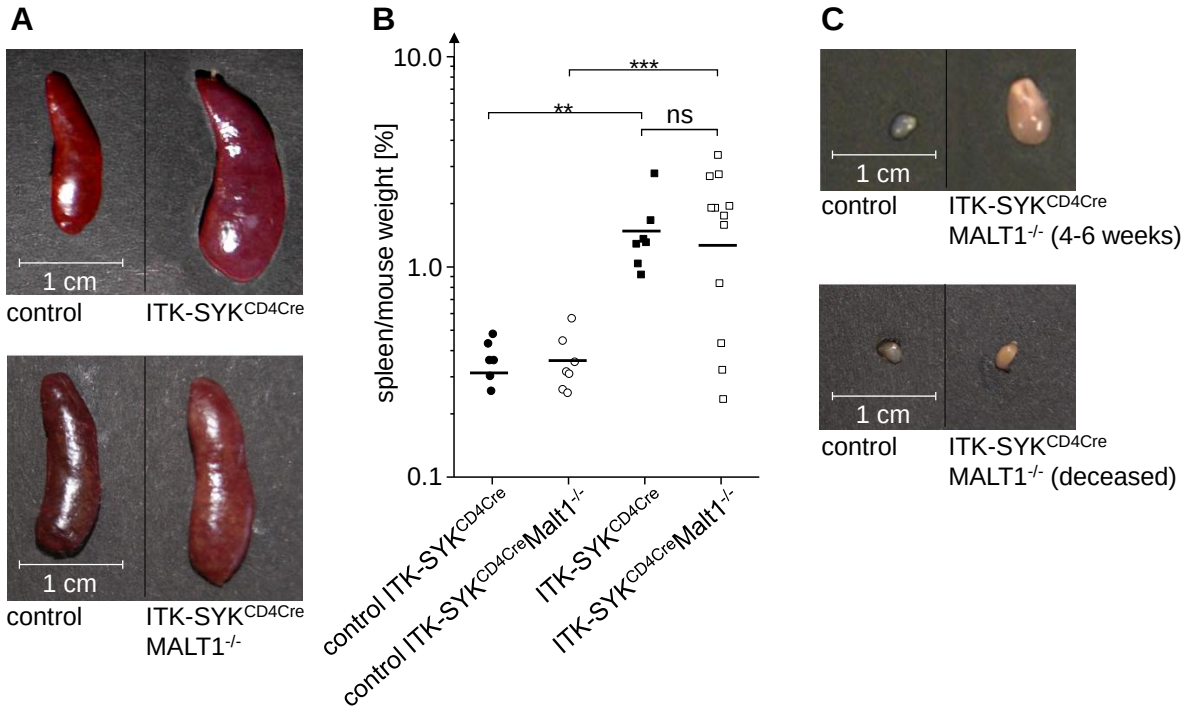

Fig. 8: Macroscopic Findings (Spleen, Lymph Node). A *One representative spleen of the indicated genotypes is shown.* ***B*** *Analysis of spleen/mouse weight ratio of deceased mice. The unpaired two-tailed Student's t test was used to analyze statistical significance (** p ≤ 0.01; *** p ≤ 0.01; not significant (ns)). Controls were defined as ITK-SYK/wildtype(wt) and CD4Cre/wt mice (referred to as control ITK-SYK^{CD4Cre}) or as MALT1$^{-/-}$ or MALT1$^{-/-}$ITK-SYK or MALT1$^{-/-}$CD4Cre mice (referred to as control ITK-SYK^{CD4Cre}MALT1$^{-/-}$). Each symbol represents an individual mouse. Horizontal bars indicate the means.* ***C*** *Representative lymph nodes from a 4-6 week old and a deceased ITK-SYK^{CD4Cre}MALT1$^{-/-}$ mouse with corresponding control.*

6.1.3 No Significant Loss of Thymocytes in Young MALT1 Deficient ITK-SYK^{CD4Cre} Mice

As outlined in 6.1.2, MALT1 absence in ITK-SYK^{CD4Cre} mice resulted in increased lymph node size. This led to the assumption, that on a genetic ITK-SYK background, MALT1 signaling was involved in thymic T-cell development.

To investigate and compare T-cell development within the thymus of ITK-SYK^{CD4Cre} and of ITK-SYK^{CD4Cre}MALT1$^{-/-}$ mice, the percental distribution and the total amount of individual thymic cell populations were determined via flow cytometry analysis.

Fig. 9 presents the representative percental distribution of the T-cell subpopulations in the thymus. Statistical analysis of the mean frequencies (data not shown) shows that both ITK-SYK genotypes have the same amount of DP T-cells as well as CD4+ T-cells. Significantly more CD8+ T-cells were determined in ITK-SYK^{CD4Cre}MALT1$^{-/-}$ mice (24.1% vs. 10.2%) but less DN T-cells (19.4% vs. 28.6%) compared to ITK-SYK^{CD4Cre} mice.

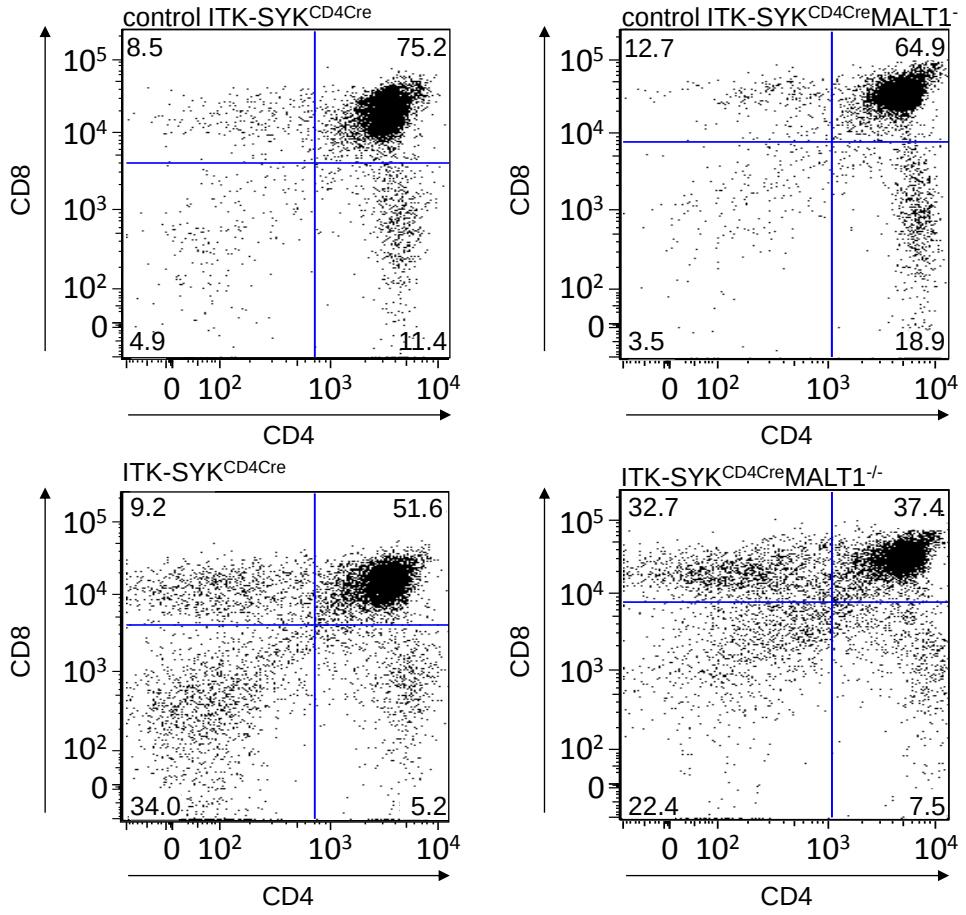

Fig. 9: Distribution of Thymocyte Subpopulations in 4-6 Week Old Mice. *Thymocytes were analyzed by flow cytometry regarding CD4 and CD8. The representative rounded figures of mice aged 4 – 6 weeks (DN, DP, CD4+ and CD8+ SP T-cells) are indicated. Data shown is representative of at least five independent experiments per genotype. Controls for ITK-SYK^{CD4Cre} mice were defined as ITK-SYK/wt or CD4Cre/wt, controls for ITK-SYK^{CD4Cre}MALT1$^{-/-}$ mice were defined as MALT1$^{-/-}$ or MALT1$^{-/-}$ITK-SYK or MALT1$^{-/-}$CD4Cre.*

For further analysis, total cell numbers in the thymus (DN, DP and SP T-cells) were determined (Fig. 10). Compared to their controls, 4 - 6 week old ITK-SYK^{CD4Cre} mice exhibited a significant loss of thymocytes which was due to a loss of DP and SP T-cells. These results were described by Pechloff *et al.* and interpreted as a result of strong ITK-SYK dependant TCR signaling leading to increased negative selection (Pechloff *et al.*, 2010).

In comparison to ITK-SYK^{CD4Cre} mice, ITK-SYK^{CD4Cre}MALT1$^{-/-}$ mice displayed significantly increased numbers of thymocytes due to accumulation of DP and SP T-cells. These results clarify that differences in lymph node size in both ITK-SYK genotypes of young age are due to a MALT1 dependant release of T-cells from the thymus.

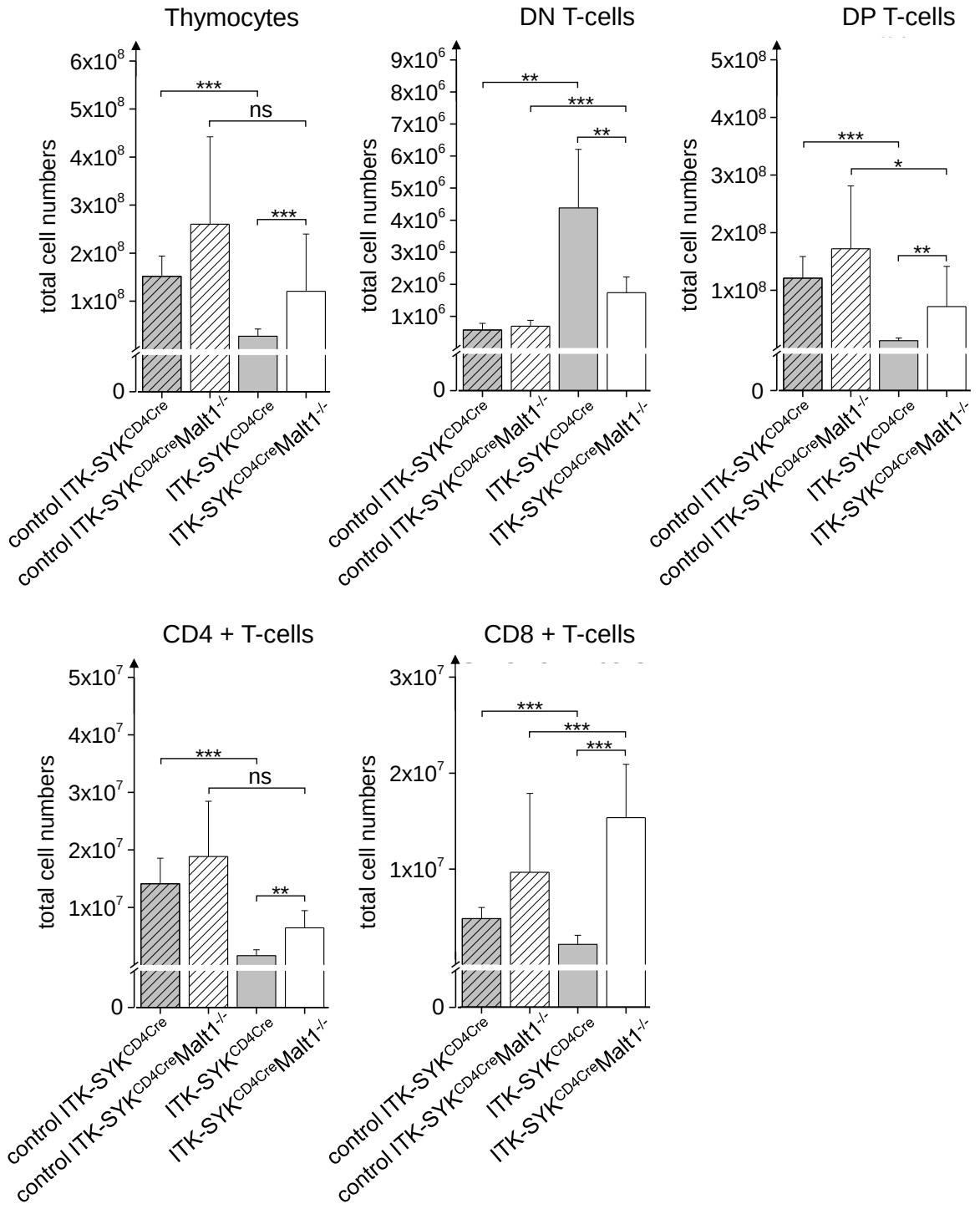

Fig. 10: Total Cell Number Analysis of Thymocytes, DP, DN and SP T-cells of young Mice in the Thymus. *Shown are the total cell numbers from thymocytes, double negative (DN), double positive (DP) and single positive (SP) T-cells with standard deviation. The unpaired two-tailed Student's t test was used to analyze statistical significance (* $p \leq 0.05$, ** $p \leq 0.01$,*** $p \leq 0.001$, not significant (ns)). Controls for ITK-SYK^{CD4Cre} mice were defined as ITK-SYK/wt or CD4Cre/wt, controls for ITK-SYK^{CD4Cre}MALT1$^{-/-}$ mice were defined as MALT1$^{-/-}$ or MALT1$^{-/-}$ITK-SYK or MALT1$^{-/-}$CD4Cre.*

6.2 Differences in T-cell Infiltration

6.2.1 No T-cell Infiltration in Lymphoid Organs in Deceased MALT1 Deficient ITK-SYK^{CD4Cre} Mice

Experiments from 6.1 had demonstrated a significant, MALT1 dependant difference concerning survival and thymic T-cell development in the ITK-SYK mouse model. To investigate whether MALT1 deficient ITK-SYK mice still presented with infiltration of lymphoid organs as a characteristic observed in PTCL, splenic and lymph node cells from deceased mice of both ITK-SYK genotypes and their controls were analyzed via flow cytometry.

Pechloff *et al.* showed the ITK-SYK^{CD4Cre} phenotype comprises of three groups of mice in terms of T-cell predominance (Pechloff *et al.*, 2010). Data obtained in this thesis confirmed results shown by Pechloff *et al.* The majority of mice (50%) developed malignant lymphoma with manifestation in spleen and lymph node with T-cells that were CD4+, the second group (37.5%) showed a vice versa scenario with upregulation of CD8. The third group (12.5%) retained both the CD4+ and CD8+ T-cell population (data not shown).

In contrast to the findings described above, ITK-SYK^{CD4Cre}MALT1$^{-/-}$ mice did not show a predominance of one specific T-cell subtype in the spleen as observed in ITK-SYK^{CD4Cre} mice. Instead, in average about 16% of all cells in the spleen were CD4+ T-cells and 9.0% were CD8+ T-cells, which equaled their corresponding controls (Fig. 11 A). Compared to ITK-SYK^{CD4Cre} mice, the analysis of total cell numbers revealed a significant loss of total T-cell numbers in ITK-SYK^{CD4Cre}MALT1$^{-/-}$ mice in the spleen (Fig. 11 B).

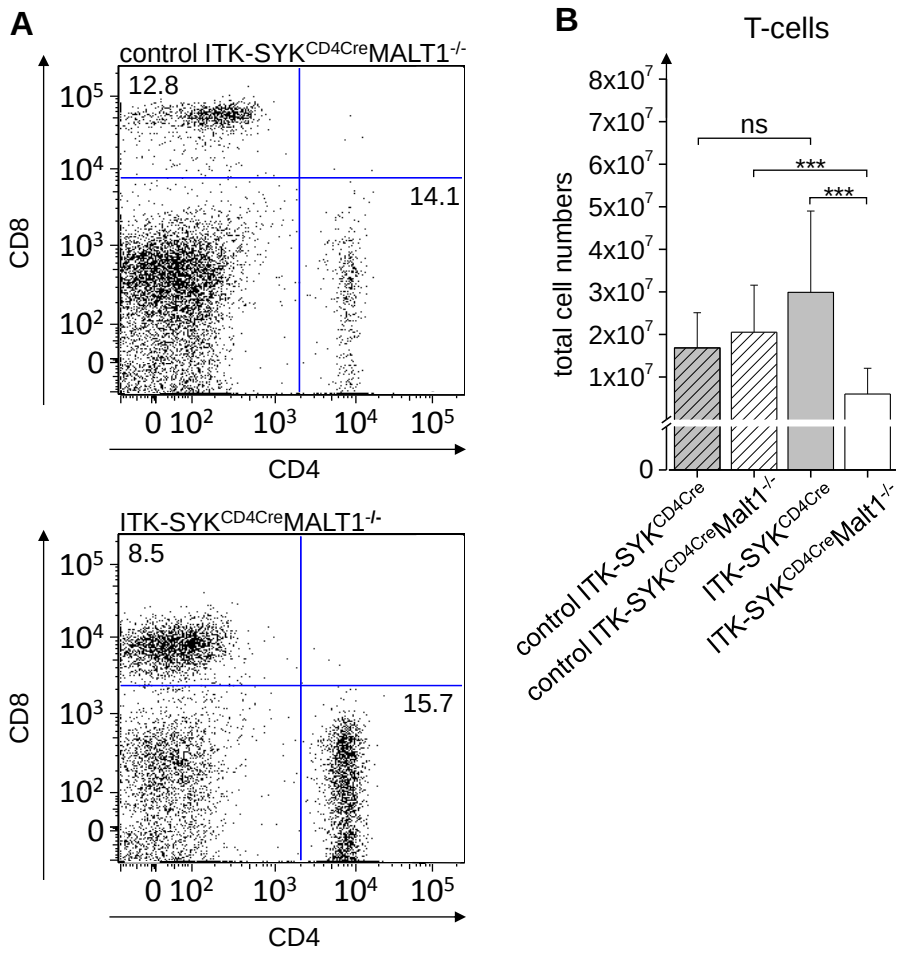

Fig. 11: Percental Distribution and Total Cell Number of Splenic CD4+ and CD8+ T-cells in Deceased Mice. A *Splenocytes were stained against CD4 and CD8 and analyzed by flow cytometry. The frequencies of two representative mice are indicated. Analyzed data resulted from eight independent experiments per genotype.* ***B*** *Shown are the total T-cell numbers and total cell numbers from CD4+ and CD8+ T-cells with standard deviation. The unpaired two-tailed Student's t test was used to analyze statistical significance (* p ≤ 0.05, *** p ≤ 0.001, not significant (ns)). Controls for ITK-SYK^{CD4Cre} mice were defined as ITK-SYK/wt or CD4Cre/wt, controls for ITK-SYK^{CD4Cre}MALT1$^{-/-}$ mice were defined as MALT1$^{-/-}$ or MALT1$^{-/-}$ITK-SYK or MALT1$^{-/-}$CD4Cre.*

In addition to analysis of the spleen, flow cytometry analysis of lymph nodes was performed equally.

Compared to corresponding controls, the percentage of CD8+ T-cells decreased from about 29.0% (control) to 16.0% in ITK-SYK^{CD4Cre}MALT1$^{-/-}$ mice. In contrast, CD4+ T-cells increased slightly from about 25.0% (control) to 30.0% (Fig. 12 A).

Compared to ITK-SYK^{CD4Cre} mice, total T-cell numbers in ITK-SYK^{CD4Cre}MALT1$^{-/-}$ mice decreased significantly, however less as observed in the spleen (Fig. 12 B).

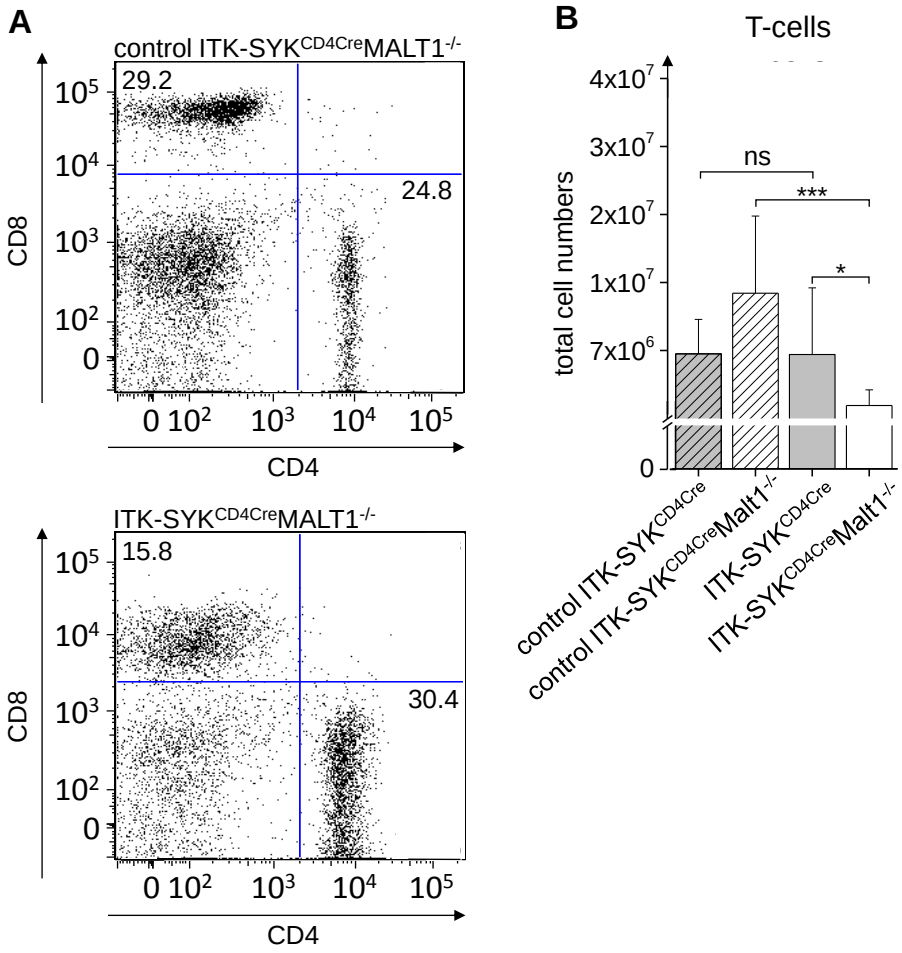

Fig. 12: Percentual Distribution and Total Cell Numbers of CD4+ and CD8+ T-cells in the Lymph Nodes of Deceased Mice. A *Lymphocytes were stained against CD4 and CD8 and analyzed by flow cytometry. The frequencies of two representative mice are indicated. Analyzed data resulted from seven independent experiments per genotype.* ***B*** *Shown are the total T-cell numbers and total cell numbers from CD4+ and CD8+ T-cells with standard deviation. The unpaired two-tailed Student's t test was used to analyze statistical significance (* $p \leq 0.05$, *** $p \leq 0.001$, not significant (ns)). Controls for ITK-SYK^{CD4Cre} mice were defined as ITK-SYK/wt or CD4Cre/wt, controls for ITK-SYK^{CD4Cre}MALT1$^{-/-}$ mice were defined as MALT1$^{-/-}$ or MALT1$^{-/-}$ITK-SYK or MALT1$^{-/-}$CD4Cre.*

As shown, ITK-SYK^{CD4Cre}MALT1$^{-/-}$ mice differed significantly from ITK-SYK^{CD4Cre} mice in terms of T-cell distribution in the lymphoid organs such as spleen and lymph nodes. Outgrowth of one specific T-cell subpopulation such as in ITK-SYK^{CD4Cre} mice, which mainly expressed CD4, was not detected on a MALT1$^{-/-}$ background. Compared to ITK-SYK^{CD4Cre} mice, total T-cell numbers in spleen and lymph nodes decreased significantly in ITK-SYK^{CD4Cre}MALT1$^{-/-}$ mice.

6.2.2 Less Severe Peripheral T-cell Infiltration in the Organs of Deceased MALT1 Deficient ITK-SYK^{CD4Cre} Mice

Pechloff *et al.* showed that deceased ITK-SYK^{CD4Cre} mice harbored a significant percentual increase of total T-cells in liver, kidney, lung and bone marrow compared to controls (Pechloff *et al.* 2010). As outlined in 6.2.1, analysis of spleen and lymph nodes from MALT1 deficient ITK-SYK^{CD4Cre} mice did not show a T-cell infiltration in these lymphoid organs. To determine the extent of T-cell infiltration in the peripheral organs (defined as liver, kidney, lung and bone marrow) as a characteristic of malignant cells, flow cytometric analysis of these tissues was performed.

Compared to ITK-SYK^{CD4Cre} mice, a significant decrease of T-cell percentages was detected in all four examined organs taken from MALT1 deficient ITK-SYK^{CD4Cre} mice (Fig. 13). Together with the findings from spleen and lymph nodes, this suggested that the extent of peripheral organ infiltration was less in MALT1 deficient ITK-SYK mice compared to ITK-SYK^{CD4Cre} mice .

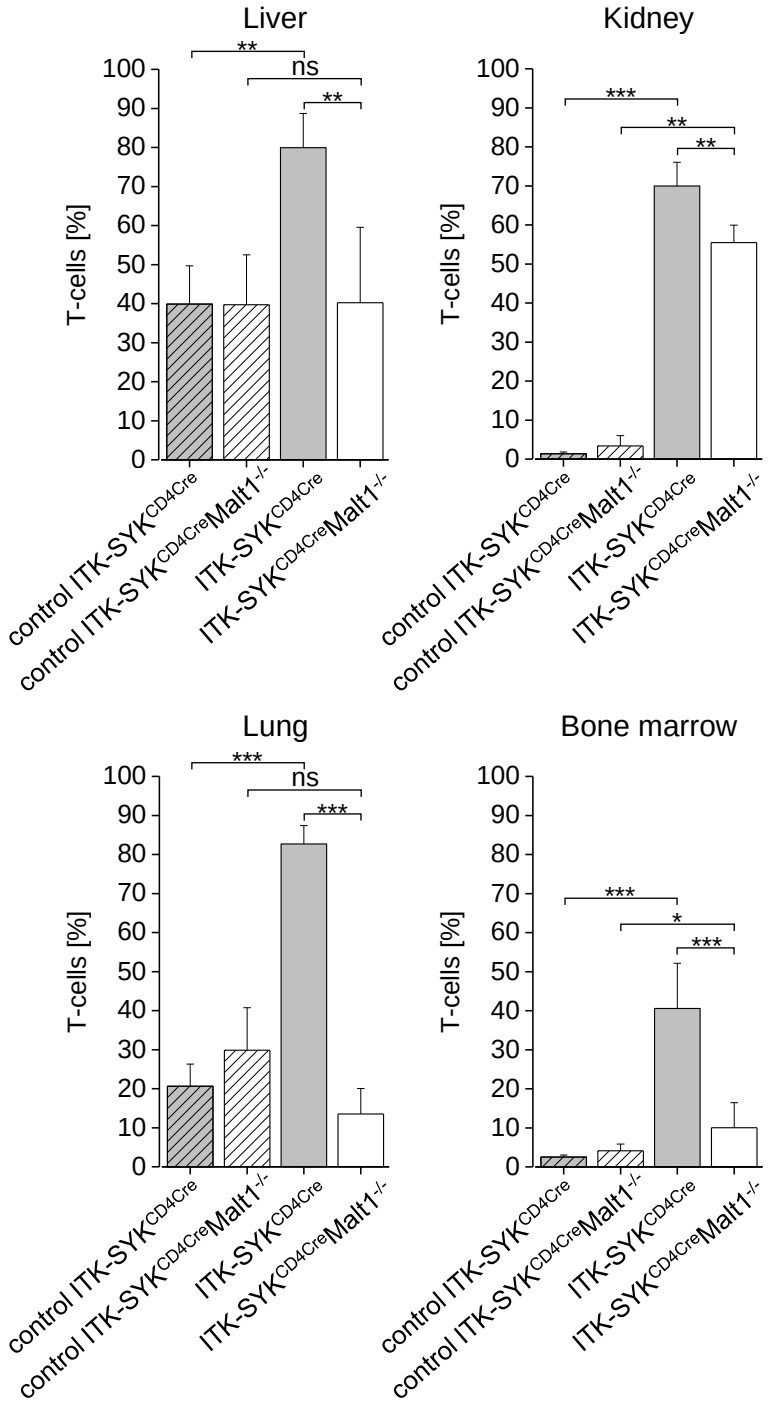

Fig. 13: Percentage of T-cells in Liver, Kidney, Lung and Bone Marrow of Deceased Mice. *Cells from the depicted organs were stained against TCR and analyzed by flow cytometry. Shown are mean values with standard deviation. Presented data resulted from at least three independent experiments. The unpaired two-tailed Student's t test was used to analyze statistical significance (* $p \leq 0.05$, ** $p \leq 0.01$, *** $p \leq 0.001$, ns (not significant)). Controls for ITK-SYK^{CD4Cre} mice were defined as ITK-SYK/wt or CD4Cre/wt, controls for ITK-SYK^{CD4Cre}MALT1$^{-/-}$ mice were defined as MALT1$^{-/-}$ or MALT1$^{-/-}$ITK-SYK or MALT1$^{-/-}$CD4Cre. Presented data resulted from five independent experiments.*

As described by Pechloff *et al.*, young ITK-SYK^{CD4Cre} animals displayed low percentages of eGFP+ lymphocytes in spleen, lymph node, bone marrow, liver, kidney and lung. Alongside with disease progression, the percentage of eGFP+ lymphocytes increased and was significantly higher in diseased animals compared to young animals. Findings from blood analysis (6.1.1) had shown that, depending on MALT1, the percentage of eGFP+ lymphocytes in the blood was either increasing (MALT$^{+/+}$) or decreasing (MALT1$^{-/-}$) over time. To see whether this was reflected in the peripheral organs as well, the development of the percentage of eGFP+ lymphocytes in young (4 - 6 weeks) and deceased animals of both ITK-SYK genotypes was compared (Fig. 14).

In young ITK-SYK^{CD4Cre}MALT1$^{-/-}$ animals, with the exception of the bone marrow, a high percentage of eGFP+ lymphocytes in the investigated organs was determined. These values did neither decrease or increase over time, with the exception of lymph nodes and bone marrow which showed increasing values. Compared to ITK-SYK^{CD4Cre} mice, deceased ITK-SYK^{CD4Cre}MALT1$^{-/-}$ mice showed significantly lower rates of eGFP+ lymphocytes with the exception of lymph nodes where the p-value was just above 0.05 (Fig. 14).

Compared to ITK-SYK^{CD4Cre} mice of the same age, 4-6 week old MALT1 deficient ITK-SYK^{CD4Cre} mice presented with significantly less percentages of peripheral T-cells and the percentage of T-cells did not increase over time. Based on these findings, it was concluded that MALT1 deficient ITK-SYK T-cells behaved less infiltrative than those on a MALT$^{+/+}$ background.

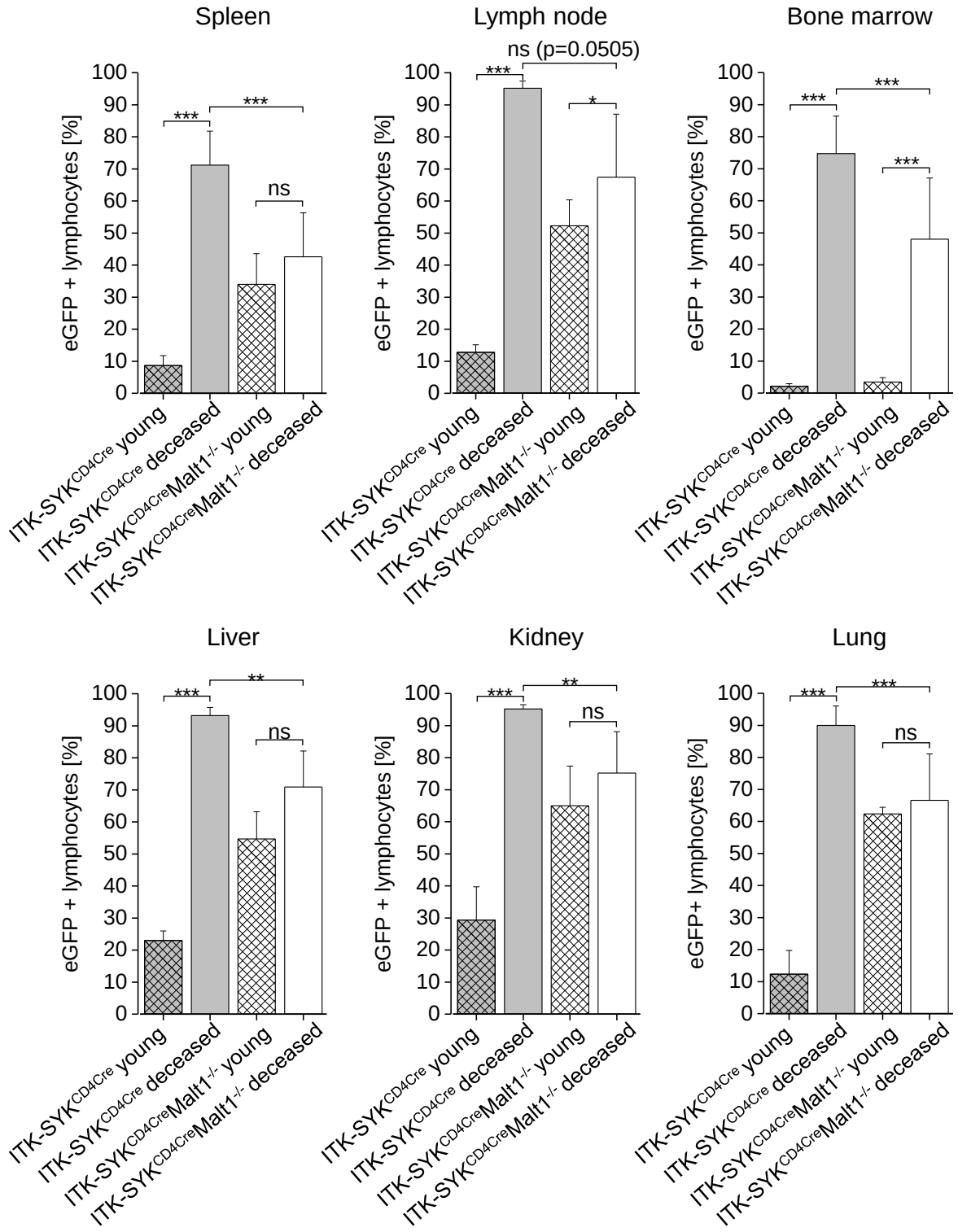

Fig. 14: Development of the Percentage of eGFP+ T-cells over Time. *eGFP was measured in lymphocytes taken from spleen, lymph node, bone marrow, liver, kidney and lung in 4-6 week old and deceased ITK-SYK^{CD4Cre} and ITK-SYK^{CD4Cre}MALT1$^{-/-}$ animals. Shown are mean values with standard deviation. Presented data resulted from at least six independent experiments. The unpaired two-tailed Student's t test was used to analyze statistical signifi-*

cance (p ≤ 0.05, ** p ≤ 0.01,*** p ≤ 0.001, not significant (ns)). Controls for ITK-SYK^{CD4Cre} mice were defined as ITK-SYK/wt or CD4Cre/wt, controls for ITK-SYK^{CD4Cre}MALT1$^{-/-}$ mice were defined as MALT1$^{-/-}$ or MALT1$^{-/-}$ITK-SYK or MALT1$^{-/-}$CD4Cre.*

6.2.3 Verification of Lymphoma in Deceased MALT1 Deficient ITK-SYK^{CD4Cre} Mice in the Lymph Nodes only

Findings from 6.1 indicated that ITK-SYK^{CD4Cre}MALT1$^{-/-}$ mice differed from ITK-SYK^{CD4Cre} mice in terms of disease outcome. For further evaluation, microscopic analysis and histological staining techniques were performed with tissue samples from skin, spleen, lymph nodes, bone marrow, liver, kidney and lung. This was done in collaboration with Professor Martina Rudelius (Department of Pathology, University of Würzburg), who performed staining and microscopic sample analysis.

In ITK-SYK^{CD4Cre} mice, two of three 4 - 6 week old mice presented with PTCL in more than one organ (Data not shown). In deceased mice, all analyzed organ samples of three individual mice from spleen, lymph node, bone marrow, liver, kidney and lung displayed lymphoma. The T-cell population was described as CD3 positive with atypical middle sized cell cores with high proliferation activity (Fig. 15 A).

The results of ITK-SYK^{CD4Cre}MALT1$^{-/-}$ mice differed. Two of three 4 - 6 week old ITK-SYK^{CD4Cre}MALT1$^{-/-}$ mice displayed PTCL, but lymph nodes were affected only. Spleen, bone marrow, liver, kidney and lung did not show abnormal T-cell populations (Data not shown). Deceased ITK-SYK^{CD4Cre}MALT1$^{-/-}$ mice displayed a granulomatous inflammation in liver, kidney, lung and conchae. Only in one out of three mice PTCL was detected and this was restricted to the lymph nodes (Fig. 15 B).

In summary, all examined organs from deceased ITK-SYK^{CD4Cre} mice displayed PTCL whereas in ITK-SYK^{CD4Cre}MALT1$^{-/-}$ mice, a granulomatous inflammation could be detected. PTCL infiltration seemed to be restricted to the lymph nodes where one of three ITK-SYK^{CD4Cre}MALT1$^{-/-}$ mice presented with PTCL . These findings confirmed observed differences in survival time,

macroscopy, T-cell analysis and eGFP+ T-cell frequencies between ITK-SYK^{CD4Cre} and ITK-SYK^{CD4Cre}MALT1$^{-/-}$ mice and suggest a less aggressive lymphoproliferative disease in ITK-SYK^{CD4Cre}MALT1$^{-/-}$ mice with additional inflammation processes which were not described in ITK-SYK^{CD4Cre} mice.

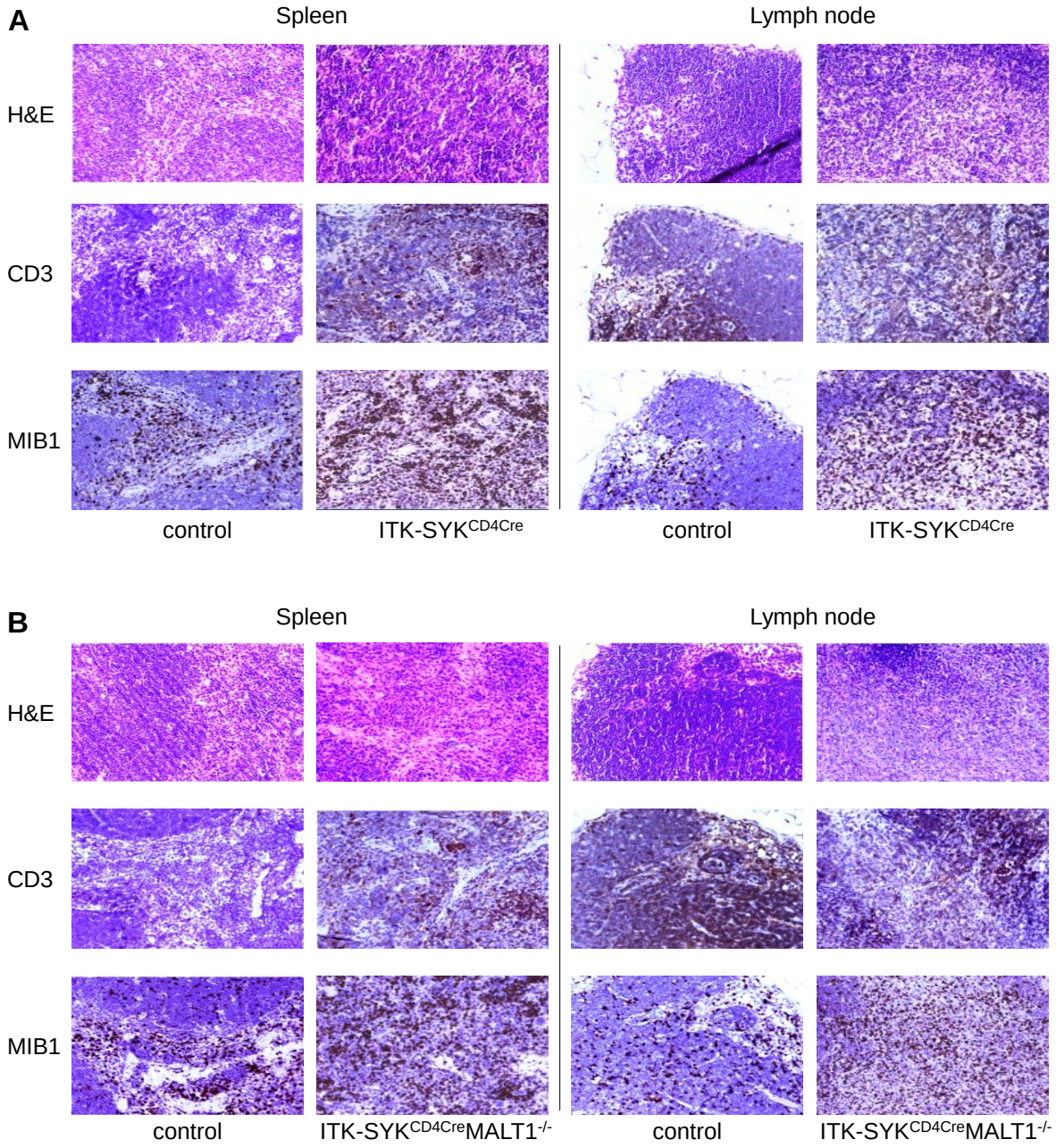

Fig. 15: Histologies of Deceased Mice from Spleen and Lymph Node. *Organs were taken from deceased mice and fixed in formaldehyde. Staining techniques: Hematoxylin and Eosin stain (H&E), CD3 antibody stain (CD3), MIB1 antibody stain against Ki-67 (MIB1).* ***A*** *Shown is one representative example of a deceased ITK-SYK^{CD4Cre} mouse with PTCL in all depicted organs.*

Controls were defined as ITK-SYK/wt or CD4Cre/wt. ***B*** *Shown is one representative example of a deceased ITK-SYK^{CD4Cre}MALT1$^{-/-}$mouse with granulomatous inflammation in all depicted organs but no confirmation of PTCL. Controls were defined as MALT1$^{-/-}$ or MALT1$^{-/-}$ITK-SYK or MALT1$^{-/-}$CD4Cre.*

6.3 Differences in T-cell Characteristics

6.3.1 T-cells from MALT1 Deficient ITK-SYK^{CD4Cre} Mice Are Activated but not Enlarged

Since disease progression was less aggressive in ITK-SYK^{CD4Cre}MALT1$^{-/-}$ mice according to findings from 6.1, more information concerning the T-cell phenotype was required. Lymphoma cells express a specific pattern of activation markers and are increased in cell size. Hence, surface expression of the activation markers, CD44 and CD62L on splenic T-cells was investigated by cell size (FSC (forward scatter)) and TCR expression. eGFP expression was used as internal control for Cre-mediated deletion of the STOP cassette and ITK-SYK gene activation.

ITK-SYK^{CD4Cre} T-cells exhibited a clearly activated phenotype with upregulation of CD44 and downregulation of CD62L in both CD4+ and CD8+ T-cells. Phenotypically, the TCR was downregulated and the T-cells were enlarged as measured by forward scatter analysis (FSC). Likewise, data generated from ITK-SYK^{CD4Cre}MALT1$^{-/-}$ mice showed an upregulation of CD44 and downregulation of CD62L in both CD4+ and CD8+ T-cells (Fig. 16 A). As a clear difference to ITK-SYK^{CD4Cre} mice, T-cells from ITK-SYK^{CD4Cre} MALT1$^{-/-}$ mice were not enlarged compared to respective controls (Fig. 16 B).

The expression profile indicated that T-cells from both genotypes displayed an activated phenotype. However, T-cells from ITK-SYK^{CD4Cre} MALT1$^{-/-}$ mice were not enlarged as demonstrated by forward scatter analysis. These findings indicated differences in T-cell activity depending on presence of MALT1 in ITK-SYK mediated signaling pathways.

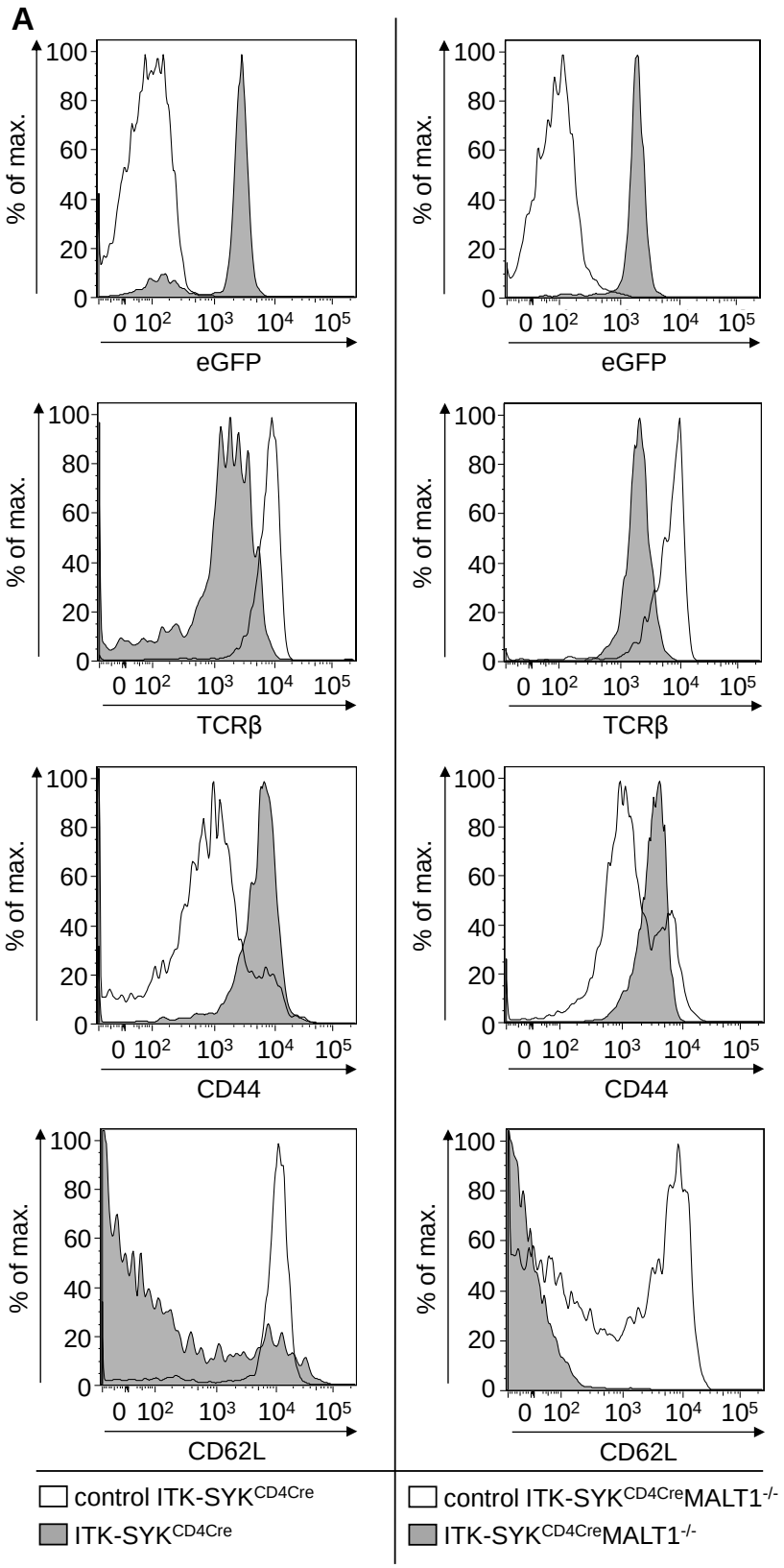
A
% of max.
100
80
60
40
20
0
0 10² 10³ 10⁴ 10⁵
eGFP
TCRβ
CD44
CD62L
control ITK-SYK^CD4Cre
ITK-SYK^CD4Cre
control ITK-SYK^CD4CreMALT1^-/-
ITK-SYK^CD4CreMALT1^-/-

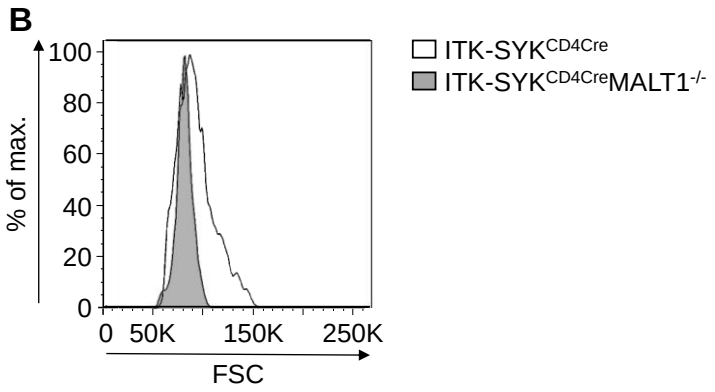

Fig. 16: T-cell Phenotype in Deceased Mice. *Splenic T-cells were stained against TCRβ, CD4, CD8, CD44 and CD62L and analyzed by flow cytometry. Shown data resulted from one representative experiment. Since no difference between CD4- and CD8+ T-cells was detected, CD4+ T-cells function as representative example. Data is true for five independent experiments.* ***A*** *T-cell phenotype of splenic ITK-SYK^{CD4Cre} and ITK-SYK^{CD4Cre} MALT1$^{-/-}$ CD4+ T-cells. Controls for ITK-SYK^{CD4Cre} mice were defined as ITK-SYK/wt or CD4Cre/wt, controls for ITK-SYK^{CD4Cre}MALT1$^{-/-}$ mice were defined as MALT1$^{-/-}$ or MALT1$^{-/-}$ ITK-SYK or MALT1$^{-/-}$CD4Cre.* ***B*** *Comparison of cell size between splenic ITK-SYK^{CD4Cre} and ITK-SYK^{CD4Cre} MALT1$^{-/-}$ CD4+ T-cells.*

6.3.2 Impaired T-cell Proliferation in MALT1 Deficient ITK-SYK^{CD4Cre} Mice

As described in 6.1, MALT1 deficiency in the ITK-SYK^{CD4Cre} mouse model resulted in a significant survival benefit. Analysis from 6.2.3 had shown that lymphoma in deceased MALT1 deficient ITK-SYK mice was restricted to the lymph nodes.

Therefore, it was of high interest to investigate the results of MALT1 deficiency on T-cell behaviour. MALT1 is described as one of the key proteins of the canonical NF-κB pathway which induces cell proliferation. Hence, an *ex vivo* proliferation assay was performed for further characterization of *ex vivo* T-cell proliferation in both ITK-SYK genotypes upon TCR stimulation.

Splenic T-cells from both ITK-SYK genotypes and corresponding controls were gathered, treated with CPD according to the manufacturer's protocol and stimulated. CPD was measured at different time points (0h, 24h, 48, 72h) by flow cytometry. At 72h, daughter cells of T-cells taken from ITK-SYK^{CD4Cre} mice could clearly be identified. In contrast, hardly no cell division could be verified in T-cells taken from ITK-SYK^{CD4Cre}MALT1$^{-/-}$ mice. This was especially the case for the CD4+ population (Fig. 17).

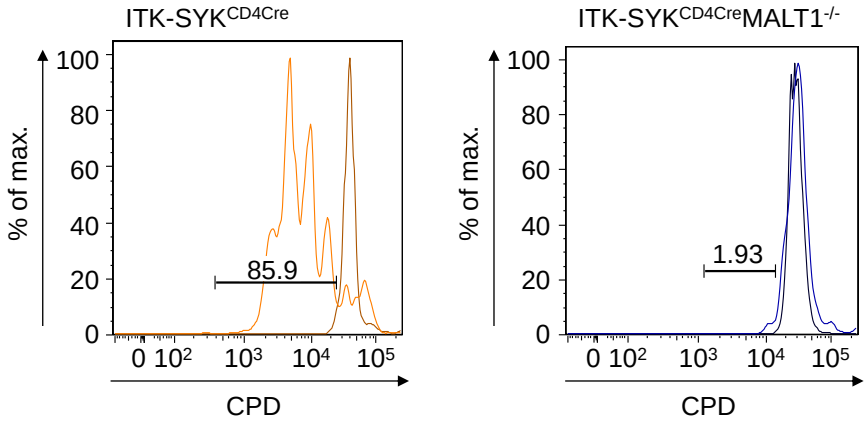

Fig. 17: Evaluation of T-cell Proliferation. *Splenic T-cells were extracted, treated with Cell Proliferation Dye (CPD) and stained against CD4 and CD8. CPD was measured at 0h, 24h, 48h and 72h by flow cytometry. Shown is one exemplary result for CD4+ T-cells from ITK-SYK^{CD4Cre} mice (left) compared with T-cells from ITK-SYK^{CD4Cre}MALT1$^{-/-}$ mice (right) at 72 h. Each peak symbolizes one generation of cell division. Figures (in %) represent the portion of daughter cells. Stimulated cells are represented in orange (left) and blue (right), unstimulated controls of the same genotype are represented in brown (left) and black (right). Shown data is representative for three independent experiments.*

Statistical analysis from the experiment's data at 72h was performed. Direct comparison of CD4+ and CD8+ T-cells from both ITK-SYK genotypes revealed that the percentage of CD4+ daughter cells from ITK-SYK^{CD4Cre}MALT1$^{-/-}$ mice was significantly smaller compared to the CD4+ T-cell population from ITK-SYK^{CD4Cre} mice (2.0% versus 12.0%). No significant difference was detected between the CD8+ T-cell populations (28.5% versus 17.0%), however there

was a trend towards lower values in CD8+ T-cells from ITK-SYK^{CD4Cre}MALT1$^{-/-}$ mice (Fig. 18).

The results from the proliferation experiments showed that MALT1 deficient ITK-SYK^{CD4Cre} T-cells proliferated significantly less than with presence of MALT1. This is consistent with findings from 6.2.2 which demonstrated that the T-cell population in MALT1 deficient ITK-SYK^{CD4Cre} did not increase over time in the peripheral organs.

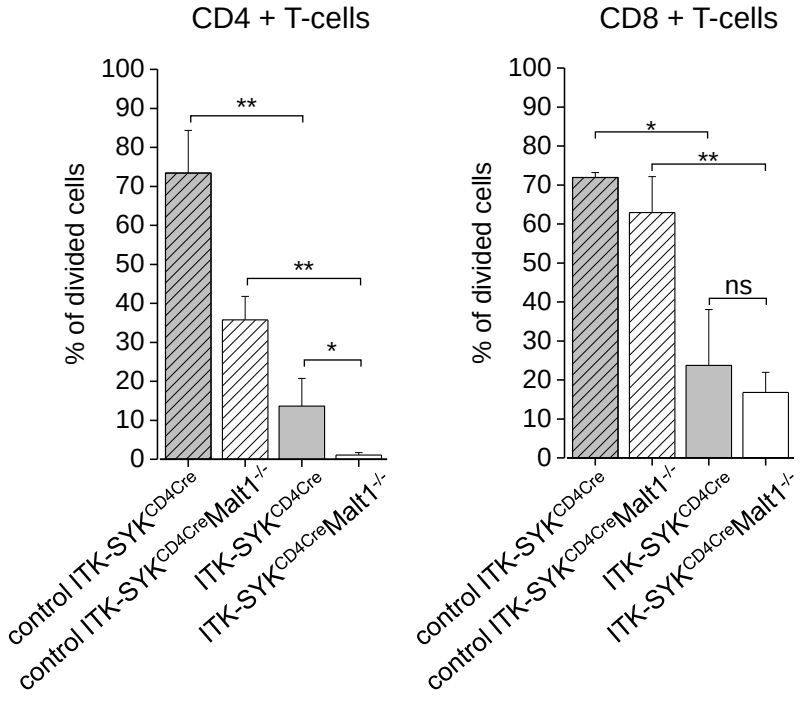

Fig. 18: Proliferative Capacity of Stimulated CD4+ and CD8+ T-cells. *Splenic T-cells were extracted, treated with CPD and stimulated with CD3/CD28. CPD intensity was measured at 72h by flow cytometry. The portion of daughter cells (see Fig. 17) from three independent experiments was taken and the unpaired two-tailed Student's t test was used to analyze statistical significance (* p ≤ 0.05, ** p ≤ 0.01, not significant (ns)). Illustrated are mean values with standard deviation. Controls for ITK-SYK^{CD4Cre} mice were defined as ITK-SYK/wt or CD4Cre/wt, controls for ITK-SYK^{CD4Cre}MALT1$^{-/-}$ mice were defined as MALT1$^{-/-}$ or MALT1$^{-/-}$ITK-SYK or MALT1$^{-/-}$CD4Cre.*

6.3.3 Increased *ex vivo* Apoptosis Rates in MALT1 Deficient ITK-SYK^{CD4Cre} T-cells

Lymphoma cells undergo modulations of apoptosis signaling resulting in higher resistance towards extra- and intracellular pro-apoptotic stimuli. To investigate whether MALT1 absence influenced apoptosis in the ITK-SYK mouse model, the apoptotic potential of T-cells from both ITK-SYK genotypes was investigated *ex vivo*. Splenic T-cells were harvested , stained against TCRβ, Annexin V and 7AAD and analyzed by flox cytometry. Both ITK-SYK genotypes showed a constant increase of the apoptotic cell population. Direct comparison between T-cells from ITK-SYK^{CD4Cre} and ITK-SYK^{CD4Cre}MALT1$^{-/-}$ mice revealed that the percentage of apoptotic T-cells was significantly higher in T-cells from ITK-SYK^{CD4Cre}MALT1$^{-/-}$ mice at 24 h and 48 h (Fig. 19).

T-cells taken from MALT1 deficient TK-SYK^{CD4Cre} mice were more prone to apoptosis than T-cells taken from TK-SYK^{CD4Cre} mice. This, together with impaired proliferation, could be one reason for the less aggressive course of PTCL in MALT1 deficient ITK-SYK^{CD4Cre} animals.

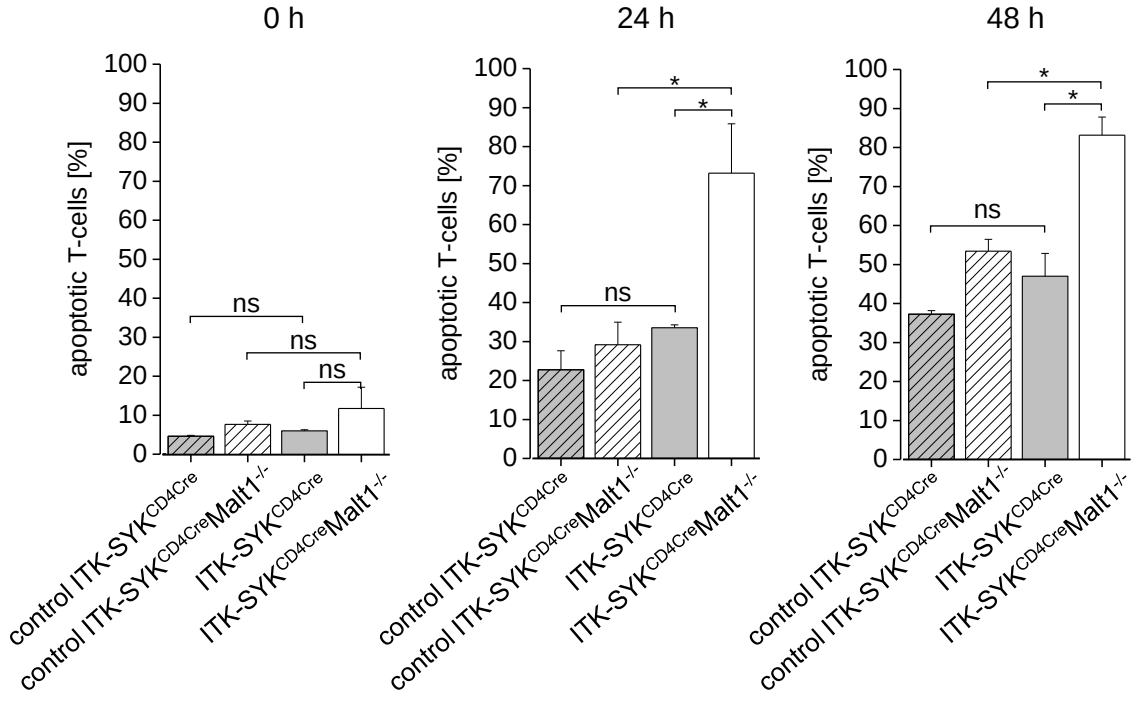

Fig. 19: Percentage of Apoptotic T-cells. *Splenic T-cells were stained against TCRβ, Annexin V and 7AAD. The apoptotic cell population was defined as Annexin V positive (early stage apoptotic stage) or Annexin V/7AAD positive (late stage apoptosic cells) and its proportion was measured at 0h, 24h and 48h. Each bar comprises three independent experiments with standard deviation, the unpaired two-tailed Student's t test was used to analyze statistical significance (* $p \leq 0.05$, not significant (ns)). Depicted are mean values with standard deviation. Controls for ITK-SYK^{CD4Cre} mice were defined as ITK-SYK/wt or CD4Cre/wt, controls for ITK-SYK^{CD4Cre}MALT1$^{-/-}$ mice were defined as MALT1$^{-/-}$ or MALT1$^{-/-}$ITK-SYK or MALT1$^{-/-}$CD4Cre.*

7 Discussion

The analysis of molecular signaling pathways in malignant T-cells adopts an important role in strategies to develop new treatment options for T-cell lymphoma. Those are strongly required since overall survival in the relapse situation, especially in PTCL-NOS, remains poor for those patients who are not eligible for stem cell transplantation. Blockage of intracellular signaling pathways such as in B-cell lymphoma therapy has not yet been described for PTCL-NOS. Identification of specific PTCL-NOS subgroups could be helpful to study the underlying biological mechanisms and identify possible target structures for a more specific therapeutic approach.

The translocation t(5;9)(q33;q22), coding for ITK-SYK, was discovered in 2006 as a subgroup of PTCL-NOS (Streubel *et al.*, 2006). A transgenic mouse model for ITK-SYK which demonstrated the development of an ITK-SYK mediated lymphoproliferative disease was published in 2010. This thesis investigates the role of MALT1 as important molecule in the NF-κB pathway downstream of proximal TCR signaling in the stated mouse model. This was done by comparison of ITK-SYK^{CD4Cre} mice and MALT1 deficient ITK-SYK^{CD4Cre} mice.

7.1 Loss of MALT1 Results in Thymic Alteration of T-cell Distribution

A clear difference between both ITK-SYK mice was the distribution of the thymic T-cell populations. In ITK-SYK^{CD4Cre}MALT1$^{-/-}$ mice, the reduction of DP T-cells was not as severe as seen in ITK-SYK^{CD4Cre} mice and resulted in normal (CD4+ T-cells) or increased (CD8+ T-cells) numbers of T-cells. Consequently, young ITK-SYK^{CD4Cre}MALT1$^{-/-}$ mice presented with enlarged lymph nodes whereas ITK-SYK^{CD4Cre} mice did not. Furthermore, in this work it was demonstrated that young ITK-SYK^{CD4Cre}MALT1$^{-/-}$ mice started with high percentages of eGFP+ T-cells in blood and organs whereas ITK-SYK^{CD4Cre} mice initially displayed low levels of eGFP+ T-cells. These results led to the conclusion that on a genetic ITK-SYK background, MALT1 was involved in deletion of thymic T-cells.

Negative selection induces apoptosis in highly self-antigen reactive T-cells to impede the presence of autoreactive T-cells in the periphery (Murphy *et al.*, 1990). As ITK-SYK mimics a strong TCR signal, on a cellular level this might be misinterpreted as a result of highly affine self-antigen recognition engaging apoptotic pathways to eliminate the cell.

Several transgenic mouse models have been developed to study the role of the NF-κB pathway in negative selection which remains ambivalent (Jost *et al.*, 2007)(Hettmann *et al.*, 1999). In the context of ITK-SYK, the findings suggest a positive role of MALT1 in negative selection processes in the thymus in ITK-SYK T-cells. In detail, the absence of MALT1 in the ITK-SYK^{CD4Cre} mouse model leads to reduced levels of deletion of thymic T-cells. Consequently, this leads to increased numbers of MALT1 deficient ITK-SYK T-cells in the periphery and enlarged lymph nodes as observed. However, it is also conceivable that absence of MALT1 leads to reduced levels of proinflammatory cytokines which might contribute to these observations, as well.

7.2 Loss of MALT1 Impedes Peripheral T-cell Infiltration

Deceased ITK-SYK^{CD4Cre} mice showed a constantly increasing infiltration into all peripheral organs consistent with a chronic lymphoma disease. The analysis of the percentage of ITK-SYK+ T-cells in all peripheral organs revealed that MALT1 deficiency led to significantly reduced numbers of lymphoma cells compared to ITK-SYK^{CD4Cre} mice. Histopathologically, lymphoma cells were confirmed in ⅓ of deceased MALT1 deficient ITK-SYK^{CD4Cre} mice only and this was restricted to the lymph nodes.

Since MALT1 is a positive regulator of T-cell survival, proliferation and activation (Ruland *et al.*, 2003), assays were performed to study the function of MALT1 in T-cells in the ITK-SYK^{CD4Cre} lymphoma mouse model. The results from these experiments showed that T-cells from ITK-SYK^{CD4Cre}MALT1$^{-/-}$ compared to ITK-SYK^{CD4Cre} mice were more prone to *ex vivo* apoptosis and hardly proliferated upon *ex vivo* stimulation. This probably suggests that signaling of ITK-SYK depends on MALT1 activity and that loss of MALT1 reduces the abil-

ity of ITK-SYK to drive certain signaling pathways. This consequently results in the loss of a continuous endogenous stimulation signal so that T-cells of ITK-SYK^{CD4Cre}MALT1$^{-/-}$ background proliferate less and tend to go into apoptosis more easily than T-cells of ITK-SYK^{CD4Cre} background. Consistent with this data, T-cells from ITK-SYK^{CD4Cre}MALT1$^{-/-}$ were not enlarged compared to T-cells from ITK-SYK^{CD4Cre} mice. This suggested an impaired tumor cell metabolism due to MALT1 loss.

Findings from blood analysis support data from proliferation and apoptosis assays. It was observed that the majority of ITKSYK^{CD4Cre}MALT1$^{-/-}$ mice initially displayed high percentages of eGFP+ lymphocytes in the blood, probably due to reduced negative selection of ITKSYK^{CD4Cre}MALT1$^{-/-}$ T-cells in the thymus. Over time, eGFP+ lymphocytes decreased constantly in the majority of ITKSYK^{CD4Cre}MALT1$^{-/-}$ mice. This can either be interpreted as an increased homing event of circulating T-cells into various organs or instead indicate a loss of peripheral ITK-SYK expressing T-cells lacking MALT1, which influences their survival capacity or apoptotic behaviour. This second theory is supported by the result that the percentage of T-cells in liver, kidney and lung in ITK-SYK^{CD4Cre}MALT1$^{-/-}$ mice were not significantly increased compared to ITK-SYK^{CD4Cre} mice.

7.3 Loss of MALT1 Results in a Different Disease Outcome and Prolonged Survival Time

The CBM complex acts as an important signaling complex to link lymphocyte activation with downstream signaling pathways that promote cellular proliferation and survival. Lymphoid malignancies are related to gain-of-function mutations in the genes encoding for the CBM proteins or their upstream regulators. Immunodeficiency is described in loss-of-function mutations (Juilland and Thome, 2016). The role of MALT1 and its paracaspase activity in specific types of B-cell lymphoma is well studied and has led to the development of MALT1 inhibitors. Especially in the activated B-cell (ABC) subtype of DLBCL, blockage of MALT1 paracaspase in preclinical studies was proven to be a

successful means to suppress cancer activity (Fontan *et al.*, 2012). Similar results for T-cell lymphoma are not published, probably due to the heterogeneity of this specific disease which is reflected in poorer survival rates compared to B-cell lymphoma.

When comparing the mouse strains of ITK-SYK^{CD4Cre} and ITK-SYK^{CD4Cre}MALT1$^{-/-}$ mice, in average ITK-SYK^{CD4Cre}MALT1$^{-/-}$ mice died at the age of 40 weeks, whereas ITK-SYK^{CD4Cre} mice died at the age of 26 weeks, indicating an important role of the signaling molecule MALT1 in the disease outcome of ITK-SYK driven PTCL.

Eventually, ITK-SYK^{CD4Cre}MALT1$^{-/-}$ mice died earlier than their corresponding controls which were on a MALT1$^{-/-}$ background. The cause of death could not be clarified entirely. However, certain findings suggested that ITK-SYK^{CD4Cre}MALT1$^{-/-}$ mice did not die of a pure lymphoma disease progression. While ITK-SYK^{CD4Cre} mice showed a chronic decline of general health conditions such as increased weight loss and lethargy, ITK-SYK^{CD4Cre}MALT1$^{-/-}$ mice rather presented with acute health deterioration within few (1 - 2) days resembling sepsis. This indicated that the death of ITK-SYK^{CD4Cre}MALT1$^{-/-}$ mice was not primarily due to lymphoma but could be due to immunodeficiency consistent with the role of MALT1 in immune response. Pathologically, in deceased ITK-SYK^{CD4Cre}MALT1$^{-/-}$ mice, lymphoma was verified in lymph nodes only. Instead, as described by the pathologist, a prominent granulomatous inflammation with abscess formation was observed.

This is in accordance with MALT1 being described as an important signaling molecule in immune signaling, especially NF-κB signaling. Loss of MALT1 is responsible for dysfunctional T-cell activation, proliferation and cytokine production. Yet, MALT1$^{-/-}$ mice do not die earlier than their wildtype controls as observed in this thesis and described (Ruland *et al.*, 2003). In this respect, it can be hypothesized that in ITK-SYK^{CD4Cre}MALT1$^{-/-}$ mice, the combination of a lymphoproliferative disease under the absence of MALT1 is promoting inflammatory signals and causes a setting with an increased response of innate im-

mune cells such as granulocytes and a less prominent spreading of malignant T-cells.

Considering the results of the performed experiments, MALT1 was identified as a key signaling molecule downstream of ITK-SYK. Tumor initiation was delayed in MALT1 deficient ITKSYK^{CD4Cre} mice with a significant survival benefit. However, it seems likely that other signaling pathways are also involved in ITK-SYK mediated lymphomagenesis since lymphoma cells were still detectable in a portion of deceased mice. As T-cell proliferation was reduced and apoptosis rates increased, it can be hypothesized that tumor maintenance could also be affected by MALT1 loss.

Since performed experiments were *ex vivo* where culturing conditions can not reflect the tumor microenvironment, further research is required. This could involve the establishment of a human ITK-SYK+ lymphoma cell line and xenograft experiments with MALT1 inhibitors. This should provide more information on clinical relevance of MALT1 paracaspase inhibition in human PTCL-NOS with proven ITK-SYK translocation.

8 List of Figures

9 List of Tables

10 Bibliography

International Peripheral T-Cell and Natural Killer/T-Cell Lymphoma Study: Pathology Findings and Clinical Outcomes (2008). In: *Journal of Clinical Oncology* 26 (25), S. 4124–4130.

Anderson, J. R.; Armitage, J. O.; Weisenburger, D. D. (1998): Epidemiology of the non-Hodgkin's lymphomas: distributions of the major subtypes differ by geographic locations. Non-Hodgkin's Lymphoma Classification Project. In: *Ann. Oncol.* 9 (7), S. 717–720.

Armitage, James O. (2012): The aggressive peripheral T-cell lymphomas: 2012 update on diagnosis, risk stratification, and management. In: *Am. J. Hematol.* 87 (5), S. 511–519. DOI: 10.1002/ajh.23144.

Baens, Mathijs; Bonsignore, Luca; Somers, Riet; Vanderheydt, Charlotte; Weeks, Stephen D.; Gunnarsson, Jenny (2014): MALT1 auto-proteolysis is essential for NF-κB-dependent gene transcription in activated lymphocytes. In: *PLoS ONE* 9 (8), S. e103774. DOI: 10.1371/journal.pone.0103774.

Beaven, Anne W.; Diehl, Louis F. (2015): Peripheral T-cell lymphoma, NOS, and anaplastic large cell lymphoma. In: *Hematology / the Education Program of the American Society of Hematology. American Society of Hematology. Education Program* 2015 (1), S. 550–558. DOI: 10.1182/asheducation-2015.1.550.

Campo, E.; Swerdlow, S. H.; Harris, N. L.; Pileri, S.; Stein, H.; Jaffe, E. S. (2011): The 2008 WHO classification of lymphoid neoplasms and beyond: evolving concepts and practical applications. In: *Blood* 117 (19), S. 5019–5032. DOI: 10.1182/blood-2011-01-293050.

Courtois, G.; Gilmore, T. D. (2006): Mutations in the NF-kappaB signaling pathway: implications for human disease. In: *Oncogene* 25 (51), S. 6831–6843. DOI: 10.1038/sj.onc.1209939.

d'Amore, F.; Gaulard, P.; Trümper, L.; Corradini, P.; Kim, W-S; Specht, L. (2015): Peripheral T-cell lymphomas: ESMO Clinical Practice Guidelines for

diagnosis, treatment and follow-up. In: *Annals of oncology : official journal of the European Society for Medical Oncology / ESMO* 26 Suppl 5, S. v108-15. DOI: 10.1093/annonc/mdv201.

Dejardin, Emmanuel (2006): The alternative NF-kappaB pathway from biochemistry to biology: pitfalls and promises for future drug development. In: *Biochem. Pharmacol.* 72 (9), S. 1161–1179. DOI: 10.1016/j.bcp.2006.08.007.

Ferlay J, Soerjomataram I, Ervik M, Dikshit R, Eser S, Mathers C, Rebelo M, Parkin DM, Forman D, Bray, F.: GLOBOCAN 2012 v1.0, Cancer Incidence and Mortality Worldwide: IARC CancerBase No. 11 [Internet]. Lyon, France: International Agency for Research on Cancer; 2013. Available from: http://globocan.iarc.fr, accessed on 28/11/2014.

Fontan, Lorena; Yang, Chenghua; Kabaleeswaran, Venkataraman; Volpon, Laurent; Osborne, Michael J.; Beltran, Elena (2012): MALT1 small molecule inhibitors specifically suppress ABC-DLBCL in vitro and in vivo. In: *Cancer cell* 22 (6), S. 812–824. DOI: 10.1016/j.ccr.2012.11.003.

Ghosh, S.; May, M. J.; Kopp, E. B. (1998): NF-kappa B and Rel proteins: evolutionarily conserved mediators of immune responses. In: *Annu Rev Immunol* 16, S. 225–260. DOI: 10.1146/annurev.immunol.16.1.225.

Golde, William T.; Gollobin, Peter; Rodriguez, Luis L. (2005): A rapid, simple, and humane method for submandibular bleeding of mice using a lancet. In: *Lab Anim (NY)* 34 (9), S. 39–43. DOI: 10.1038/laban1005-39.

Hettmann, T.; DiDonato, J.; Karin, M.; Leiden, J. M. (1999): An essential role for nuclear factor kappaB in promoting double positive thymocyte apoptosis. In: *J. Exp. Med.* 189 (1), S. 145–158.

Hirve, Nupura; Levytskyy, Roman M.; Rigaud, Stephanie; Guimond, David M.; Zal, Tomasz; Sauer, Karsten (2012): A Conserved Motif in the ITK PH-Domain Is Required for Phosphoinositide Binding and TCR Signaling but Dispensable for Adaptor Protein Interactions. In: *PLoS ONE* 7 (9), S. e45158. DOI: 10.1371/journal.pone.0045158.

Iqbal, Javeed; Wright, George; Wang, Chao; Rosenwald, Andreas; Gascoyne, Randy D.; Weisenburger, Dennis D. (2014): Gene expression signatures delineate biological and prognostic subgroups in peripheral T-cell lymphoma. In: *Blood* 123 (19), S. 2915–2923. DOI: 10.1182/blood-2013-11-536359.

Janeway, Charles (2008): Janeway's immunobiology. 7. Aufl. New York: Garland Science.

Jaworski, Maike; Thome, Margot (2016): The paracaspase MALT1: biological function and potential for therapeutic inhibition. In: *Cellular and molecular life sciences : CMLS* 73 (3), S. 459–473. DOI: 10.1007/s00018-015-2059-z.

Jost, Philipp J.; Weiss, Stephanie; Ferch, Uta; Gross, Olaf; Mak, Tak W.; Peschel, Christian; Ruland, Jurgen (2007): Bcl10/Malt1 signaling is essential for TCR-induced NF-kappaB activation in thymocytes but dispensable for positive or negative selection. In: *J Immunol* 178 (2), S. 953–960.

Juilland, Mélanie; Thome, Margot (2016): Role of the CARMA1/BCL10/MALT1 complex in lymphoid malignancies. In: *Current opinion in hematology* 23 (4), S. 402–409. DOI: 10.1097/MOH.0000000000000257.

Klemm, Stefanie; Gutermuth, Jan; Hültner, Lothar; Sparwasser, Tim; Behrendt, Heidrun; Peschel, Christian (2006): The Bcl10-Malt1 complex segregates Fc epsilon RI-mediated nuclear factor kappa B activation and cytokine production from mast cell degranulation. In: *The Journal of experimental medicine* 203 (2), S. 337–347. DOI: 10.1084/jem.20051982.

Koopman, G.; Reutelingsperger, C. P.; Kuijten, G. A.; Keehnen, R. M.; Pals, S. T.; van Oers, M. H. (1994): Annexin V for flow cytometric detection of phosphatidylserine expression on B cells undergoing apoptosis. In: *Blood* 84 (5), S. 1415–1420.

Lee, P. P.; Fitzpatrick, D. R.; Beard, C.; Jessup, H. K.; Lehar, S.; Makar, K. W. (2001): A critical role for Dnmt1 and DNA methylation in T cell development, function, and survival. In: *Immunity* 15 (5), S. 763–774.

Li, Qiutang; Verma, Inder M. (2002): NF-κB regulation in the immune system. In: *Nat Rev Immunol* 2 (10), S. 725–734. DOI: 10.1038/nri910.

Liao, X. C.; Littman, D. R. (1995): Altered T cell receptor signaling and disrupted T cell development in mice lacking Itk. In: *Immunity* 3 (6), S. 757–769.

Longmore, J. M.; Wilkinson, Ian; Török, Estée (2001): Oxford handbook of clinical medicine. 5. Aufl. Oxford, New York: Oxford University Press.

Lucas, P. C.; Yonezumi, M.; Inohara, N.; McAllister-Lucas, L. M.; Abazeed, M. E.; Chen, F. F. (2001): Bcl10 and MALT1, independent targets of chromosomal translocation in malt lymphoma, cooperate in a novel NF-kappa B signaling pathway. In: *J Biol Chem* 276 (22), S. 19012–19019. DOI: 10.1074/jbc.M009984200.

Matsumoto, Reiko; Wang, Donghai; Blonska, Marzenna; Li, Hongxiu; Kobayashi, Masayuki; Pappu, Bhanu et al. (2005): Phosphorylation of CARMA1 plays a critical role in T Cell receptor-mediated NF-kappaB activation. In: *Immunity* 23 (6), S. 575–585. DOI: 10.1016/j.immuni.2005.10.007.

McAllister-Lucas, L. M.; Baens, M.; Lucas, P. C. (2011): MALT1 Protease: A New Therapeutic Target in B Lymphoma and Beyond? In: *Clinical Cancer Research* 17 (21), S. 6623–6631. DOI: 10.1158/1078-0432.CCR-11-0467.

Murphy, K. M.; Heimberger, A. B.; Loh, D. Y. (1990): Induction by antigen of intrathymic apoptosis of CD4+CD8+TCRlo thymocytes in vivo. In: *Science* 250 (4988), S. 1720–1723.

Nabel, G. J.; Verma, I. M. (1993): Proposed NF-kappa B/I kappa B family nomenclature. In: *Genes Dev.* 7 (11), S. 2063.

Neurauter, Axl A.; Bonyhadi, Mark; Lien, Eli; Nøkleby, Lars; Ruud, Erik; Camacho, Stephanie; Aarvak, Tanja: Cell Isolation and Expansion Using Dynabeads ®, Bd. 106, S. 41–73.

Oeckinghaus, Andrea; Wegener, Elmar; Welteke, Verena; Ferch, Uta; Arslan, Seda Cöl; Ruland, Jürgen et al. (2007): Malt1 ubiquitination triggers NF-

kappaB signaling upon T-cell activation. In: *EMBO J.* 26 (22), S. 4634–4645. DOI: 10.1038/sj.emboj.7601897.

Pahl, H. L. (1999): Activators and target genes of Rel/NF-kappaB transcription factors. In: *Oncogene* 18 (49), S. 6853–6866. DOI: 10.1038/sj.onc.1203239.

Pechloff, Konstanze; Holch, Julian; Ferch, Uta; Schweneker, Marc; Brunner, Kristina; Kremer, Markus et al. (2010): The fusion kinase ITK-SYK mimics a T cell receptor signal and drives oncogenesis in conditional mouse models of peripheral T cell lymphoma. In: *J. Exp. Med.* 207 (5), S. 1031–1044. DOI: 10.1084/jem.20092042.

Pertoft, H.; Laurent, T. C.; Låås, T.; Kågedal, L. (1978): Density gradients prepared from colloidal silica particles coated by polyvinylpyrrolidone (Percoll). In: *Anal. Biochem.* 88 (1), S. 271–282.

Rabinovitch, P. S.; Torres, R. M.; Engel, D. (1986): Simultaneous cell cycle analysis and two-color surface immunofluorescence using 7-amino-actinomycin D and single laser excitation: applications to study of cell activation and the cell cycle of murine Ly-1 B cells. In: *J. Immunol.* 136 (8), S. 2769–2775.

Ruland, J.; Duncan, G. S.; Elia, A.; del Barco Barrantes, I.; Nguyen, L.; Plyte, S. et al. (2001): Bcl10 is a positive regulator of antigen receptor-induced activation of NF-kappaB and neural tube closure. In: *Cell* 104 (1), S. 33–42.

Ruland, Jürgen; Duncan, Gordon S.; Wakeham, Andrew; Mak, Tak W. (2003): Differential requirement for Malt1 in T and B cell antigen receptor signaling. In: *Immunity* 19 (5), S. 749–758.

Sada, K.; Takano, T.; Yanagi, S.; Yamamura, H. (2001): Structure and function of Syk protein-tyrosine kinase. In: *J. Biochem.* 130 (2), S. 177–186.

Savage, Kerry J. (2005): Aggressive peripheral T-cell lymphomas (specified and unspecified types). In: *Hematology Am Soc Hematol Educ Program*, S. 267–277. DOI: 10.1182/asheducation-2005.1.267.

Sen, R.; Baltimore, D. (1986): Multiple nuclear factors interact with the immunoglobulin enhancer sequences. In: *Cell* 46 (5), S. 705–716.

Sen, Ranjan; Baltimore, David (2006): Multiple nuclear factors interact with the immunoglobulin enhancer sequences. Cell 1986. 46: 705-716. In: *J Immunol* 177 (11), S. 7485–7496.

Streubel, B.; Vinatzer, U.; Willheim, M.; Raderer, M.; Chott, A. (2006): Novel t(5;9)(q33;q22) fuses ITK to SYK in unspecified peripheral T-cell lymphoma. In: *Leukemia* 20 (2), S. 313–318. DOI: 10.1038/sj.leu.2404045.

Swerdlow, Steven H. (2008): WHO classification of tumours of haematopoietic and lymphoid tissues. 4. Aufl. Lyon, France: International Agency for Research on Cancer (World Health Organization classification of tumours).

Wiestner, Adrian (2015): The role of B-cell receptor inhibitors in the treatment of patients with chronic lymphocytic leukemia. In: *Haematologica* 100 (12), S. 1495–1507. DOI: 10.3324/haematol.2014.119123.

11 Acknowledgements

First of all, I would like to thank Professor Dr. Jürgen Ruland for giving me the chance to be part of his research group and his good advice and support.

Secondly, I would like to thank Dr. Konstanze Pechloff. Without her tutorship and constant advice this work would not have been possible.

Thirdly, a big thank you goes to the members of AG Ruland for good advice and practical help, in particular Kristina Brunner, Dr. Andreas Gewies, Dr. Oliver Gorka, Dr. Nathalie Knies and Dr. Stefan Wanninger.

I would also like to thank my collaboration partner Professor Dr. Martina Rudelius for pathological analysis and Professor Dr. Christoph Schmid for final encouragement.

Finally I would like to thank Johannes and my parents for support and sympathy.